Controlling the Structure, Dynamics, and Rheology of Colloidal Gels with Active Motion

by

Megan Szakasits

A dissertation submitted in partial fulfillment
of the requirements for the degree of
Doctor of Philosophy
(Chemical Engineering)
in the University of Michigan
2018

Doctoral Committee:

Professor Michael J. Solomon, Chair
Professor Sharon C. Glotzer
Professor Ronald G. Larson
Associate Professor Xiaoming Mao

Megan E. Szakasits

meganesz@umich.edu

ORCID iD: 0000-0002-0290-8421

Dedication

To papa, forever my numero uno and my biggest supporter

Acknowledgements

I am very thankful to all of the people that have helped me during my time in grad school, including the professors in the ChE department, my collaborators, administrative staff in the ChE department (especially Susan Hamlin and Mary Beth Westin), and my friends and family. Moving to Michigan was a difficult adjustment for me, but during my time in grad school, I was fortunate to have met so many great people that helped me along the way.

First, I would like to thank my advisor, Mike Solomon. I am certain the harsh Michigan winters would have scared me away if I weren't Mike's student. Ever since the first summer that I started in Mike's group, Mike has always been very supportive and helped me develop my skills as a researcher, collaborator, and leader. Mike was always patient whenever I was struggling, but knew when to push me whenever I needed the encouragement. Looking back, I have grown so much as a scientist because of Mike. Because of my experience in Mike's group, I developed many skills, both inside and outside of science, that give me confidence in my ability to have a positive impact on the scientific community in the future. Thank you very much Mike, I am very appreciative of everything you've done, and I feel very fortunate to have had you as my advisor.

I would also like to thank my committee members, Sharon Glotzer, Ron Larson, and Xiaoming Mao. My first exposure to soft matter was during the summer REU I did as an undergraduate in Sharon Glotzer's lab. Because of that experience, I decided to attend graduate school at Michigan. I am thankful to Sharon for welcoming me to her

Table of Contents

List of Figures

ix

List of Tables

List of Appendices

Abstract

In this dissertation, we investigate the connection between the microscopic structure and dynamics and the macroscopic rheology of gels. We study two different types of gels – fractal cluster gels made of polystyrene colloids and psyllium polysaccharide gels. Fractal cluster colloidal gels are a well characterized, model gel system, and they are technologically relevant for industrial applications of colloids. Exploring the effects of embedded active matter in colloidal gels is of scientific interest to improve the understanding of activity on disordered solids and of technological interest for the design of reconfigurable materials with multi-state mechanical properties.

In chapter two, we examine the microscopic dynamics of fractal cluster colloidal gels embedded with active matter. We prepare gels by adding a divalent salt to a suspension of polystyrene and Janus colloids, which allows the Janus colloids to be incorporated into the gel structure during gelation. We developed a novel experimental set-up that utilizes a hydrogel membrane to controllably deliver hydrogen peroxide – a fuel that drives diffusiophoretic motion of the active Janus colloids – to the gel without disrupting the gel structure. Using this set-up, we were able to measure the dynamics of the gel network before and after addition of active motion. We find the addition of active motion to colloidal gels leads to an increase (as large as a factor of 3) in the dynamics of all particles in the gel network; the amount of increase is a function of the ratio of active to passive colloids and the energy of the active colloids – which is set by the concentration of hydrogen peroxide in our experiments. We successfully model the

amount of enhancement by accounting for the direct motion of the active colloids and the indirect contribution due to the strain field that the displacement of the active colloids induces on the gel network.

In chapter three, we explore how the increase in dynamics is correlated to mechanical properties of the gel network. We produce the gels by preparing a solution of polystyrene and Janus colloids, adding hydrogen peroxide to activate the Janus colloids, and then adding divalent salt to induce gelation. We designed an experimental approach that combines anti-foam chemicals and oxygen permeable surfaces of rheometer fixtures to suppress the formation of oxygen bubbles (a disruptive by-product of the mechanism for generating active motion) during rheology measurements. We find the incorporation of active matter to colloidal gels leads to a decrease in the viscoelastic moduli of the gels. We measure the moduli as a function of the total active energy, and find the moduli of the gels decrease (by up to a factor of 8.5) with increasing active particle energy. We explore the connections between the microscopic dynamics and macroscopic rheology through microrheology measurements of the passive and active gels. We find that microrheology does not accurately predict the viscoelastic moduli of the active gels, which suggests a violation of the fluctuation dissipation theorem for our active gels. We also explore potential mechanisms that describe the effects of the activity on the gel structure and the effects of activity acting to change the dynamics of the gel.

In chapter four, we characterize the relationship between gel stability, mechanical properties, and hydration kinetics of psyllium polysaccharide gels. Psyllium is a hydrophilic polysaccharide derived from plant seeds and is most commonly used as a dietary supplement. Psyllium powders can readily absorb water and swell to form a gel,

which makes them useful as gelators or thickeners in industrial applications. The kinetic process of hydration and gelation of these gels is not well characterized or understood. Our objective was to characterize the relationship between hydration kinetics, gel stability, and mechanical rheology of psyllium gels. We present a novel technique to quantify the hydration kinetics by incorporating a fluorescent dye that binds to psyllium and allows us to image the grains during hydration. We find a correlation between gel stability and transient rheological measurements; samples prone to consolidation also had lower viscosity at short times, when the hydration process is most active. While the hydration kinetics did not show significant differences between the three psyllium materials, we find the time scales to reach plateau values in the viscosity and viscoelastic moduli are comparable to timescales observed in multi-grain hydration experiments.

Chapter 1 Introduction

1.1 Colloidal dynamics – Brownian and active motion

Colloids are small particles on the size scale between several nanometers and microns dispersed in a fluid medium. Colloids are sufficiently small that the fluid molecules exert forces on the suspended particle causing it to undergo Brownian motion [1]. The collisions of fluid molecules with the colloidal particle is an equilibrium process, with characteristic energy given by, k_BT where k_B is Boltzmann's constant and T is the temperature [1,2]. Colloids are also sufficiently large that their motion is described by continuum transport equations with stochastic features describing Brownian motion [1,3]. The ratio of thermal energy to the viscous drag forces gives the particle's diffusivity, $D = \frac{k_BT}{6\pi\mu a^2}$, where µ is the viscosity of the solvent and a is the particle radius. The diffusivity of a particle is related to the mean squared displacement through:

$$< x^2(\tau) > = 2nD\tau \tag{1}$$

where n is the dimensionality, D is the translational diffusion coefficient, and τ is lag time. The brackets in equation 1 denote an ensemble-averaged quantity. The ensemble averaged mean squared displacement is a measure of the dynamics of a colloidal particle and can be determined through experimental measurements, such as particle tracking with microscopy or dynamic light scattering [3,4].

1.1.1 Active motion

Active colloids are driven out of equilibrium through externally applied fields or energy sources and are able to convert that energy into locomotion [5]. Nature provides many examples of active motion ranging from microscopic examples such as the actin filaments of the cytoskeleton or bacterial colonies to flocks of birds or schools of fish on the macroscopic scale [6–9]. The complex, emergent behavior of active assemblies in nature has inspired the creation of synthetic active motion on the nano and micron scale [6,10]. Several mechanisms exist to generate active motion within a colloidal suspension, such as self-diffusiophoresis, electrophoresis, bubble propulsion, and Marangoni effects, amongst others [5,10,11]. These mechanisms rely on external energy sources such as light, external electric fields, or chemical reactions to generate a local gradient around the particle causing the particles to move in response [5,10].

In self-diffusiophoretic swimmers, composition, temperature or electric field gradients are induced by particle surface properties, which causes net propulsion of the particle [10]. These gradients lead to a gradient in interfacial pressure surrounding the particles. In order to balance the pressure, a solvent flow is induced, which propels the particle [12]. Howse et. al. developed a synthetic micro-swimmer that utilizes a chemical reaction at the particle surface for propulsion through self-diffusiophoresis [13]. When platinum coated polystyrene Janus spheres are suspended in a solution of hydrogen peroxide (H_2O_2), platinum catalyzes the decomposition of H_2O_2 into water and oxygen. The asymmetry of the Janus particles causes a concentration gradient around the platinum and polystyrene halves of the particles, which leads to self-propulsion [12,13]. The

propulsion speed exhibited by the particles increases with increasing H_2O_2 concentration [13,14].

1.1.2 Active colloidal dynamics and energy

At a single particle level, active motion leads to self-propulsion [13]. The propulsion speed of an active colloid can be determined through a measurement of the mean-squared displacement. The two dimensional mean-squared displacement of an active colloid is shown as ΔL^2 in equation 2, where D is the diffusivity, V is the velocity, and τ_R is the characteristic timescale of rotational diffusion [13].

$$\Delta L^2 = 4D\Delta t + \frac{V^2 \tau_R^2}{2}\left[\frac{2\Delta t}{\tau_R} + \exp\left(-\frac{2\Delta t}{\tau_R}\right) - 1\right] \tag{2}$$

At short times, the mean squared displacement scales with the active colloid velocity, $\Delta L^2 = 4D\Delta t + V^2 \Delta t^2$ for $t \ll \tau_R$ and at long times scales, the rotational diffusion causes the direction of propulsion to randomize resulting in a random walk, $\Delta L^2 = (4D + V^2 \tau_R)\Delta t$ [13]. The short time limiting form of the mean squared displacement captures the ballistic motion of active colloids, while the effects of Brownian motion are captured at long times.

While passive colloidal dynamics are driven by thermal energy, active motion is driven by external energy inputted into the system [15]. The energy of an active particle is given by, $E_A = \xi V l$, where ξ is the hydrodynamic drag coefficient, V is the velocity of a free active colloid, and l is the active particle run length, given by $l = \tau_R V$ [15]. The velocity of a free active colloid can be determined through measurements of the active particle mean squared displacement.

1.2 Colloidal assembly and gelation

1.2.1 Colloidal interactions

Colloids interact either attractively, through interactions such as depletion and Van der Waals, or repulsively, through electrostatic interactions or hard-core excluded volume repulsion [16]. These interactions can be modeled through pair potentials, which describe the attraction strength, $u(r)$, between two particles as a function of their separation distance, r. Except at very small separations, the interactions between colloidal particles are commonly well described by the DLVO potential, which incorporates attractive Van der Waals, $u_{vdw}(r)$, and repulsive electrostatic interactions, $u_{charge}(r)$ [17,18]. The Van der Waals interaction energy between two spheres of radius, R, is given by:

$$u_{vdw}(r) = -\frac{AR}{12r} \tag{3}$$

where A is the Hamaker constant. The Hamaker constant is a function of the refractive index (n) and dielectric permittivity (ε) of the colloidal particle and the medium in which the particle is suspended [16]. Typical values of the Hamaker constant for latex particles suspended in water are $A \sim 10^{-20}$ J [16].

Electrostatic interactions are described by the electric double layer interaction potential.

$$u_{charge}(r) = \frac{k_B T Z^2 \lambda_B}{(1+\kappa R)^2} \frac{\exp{(-\kappa(r-2R))}}{r} \tag{4}$$

The electrostatic potential is a function of the Debye length, κ^{-1}, interaction constant, Z, and the Bjerrum length, λ_B [16]. The Debye length and Bjerrum length are both related properties of the solvent; whereas the interaction constant is related to properties of the

particle. The Debye length describes the length of the diffuse electric double layer and is a function of the electrolyte concentration and valency. The interaction constant, Z, describes the particle's charge [16]. The equation is well-established for monovalent ions and small surface potentials.

1.2.2 Self-assembly and gelation

Self-assembly refers to the spontaneous organization of particles into ordered structures [19,20], such as crystals [21,22], glasses [23,24], and gels [25,26]. The type of assembled structure formed depends on design parameters such as the shape and chemical features of the particle [27], the inter-particle interactions, and the environment [28]. Tuning these design parameters could allow for the formation of assemblies with interesting optical or mechanical properties, such as close packed crystalline structures with structural color [29] or open network structures for enhanced rigidity at low particle density [30,31].

Colloidal gels are a self-assembled structure that form when particles have strong, but short ranged, attractive interactions [24,26,32]. Gelation can occur through several mechanisms including, arrested phase separation, percolation, kinetic arrest, or arrested spinodal decomposition [32,33]. The nature of the colloidal gelation transition – from solid-like to fluid-like properties – depends on the strength and range of the interparticle interactions as well as the colloidal volume fraction. Diffusion-limited cluster aggregation (DLCA) gels are a well understood, limiting case of disordered solids [26]. DLCA gels form when particles encounter each other, through diffusion, and bind irreversibly upon contact [24]. The same aggregation kinetics are applied to cluster-cluster interactions as the aggregation progresses in time [26].

The structure of DLCA gels can be characterized with the radial distribution function, $g(r)$, which is a measure of the probability of finding another particle at a distance, r, from a given particle [34–36]. The radial distribution function can be calculated in real space from positions of particles or measured from scattering experiments, which characterize the structure factor, $S(q)$; $S(q)$ and $g(r)$ are Fourier transform pairs, meaning $g(r)$ can be computed through a Fourier transform of the structure factor [34]. For fractal gels, $g(r)$ contains information about the gel structure, such as the fractal dimension, d_f, and average cluster size, R_c. The typical value of d_f for DLCA fractal gels is 1.8. For small separation distances, $g(r)$ scales as a power law, $g(r) \sim r^{d_f-3}$. For larger separations $(r > 4R)$, $g(r)$ can be described with a stretched exponential function:

$$g(r) = \frac{c}{R^{d_f}} r^{d_f-3} \exp\left(-\left(\frac{r}{\xi}\right)^{\gamma}\right) \tag{5}$$

where R is the particle radius, γ is the cut-off exponent, ξ is the cut-off length, which is proportional to the cluster size, and c is a pre-factor related to the density of particles within a cluster [35].

1.2.3 Active colloids and assembly

The introduction of active motion into colloidal gels, or other self-assembled structures, could allow for the creation of dynamic and reconfigurable structures. Simulations and experiments have shown that active particles can form complex assemblies that would not be accessible with particles undergoing Brownian motion. Examples include living crystals of light activated colloidal particles [7,8], rotating crystals of rotating, gear-like particles [37], and flexible filaments of magnetic self-

propelled particles [38]. Mixtures of active and passive particles have led to the formation of dynamic assemblies such as swarming and transient lane formation from mixtures of active and passive rods [39]. Active particles have also been used to alter the equilibrium structures formed by passive, Brownian particles. Active particles have been used to enhance the crystallinity of polycrystalline samples by removing grain boundaries [40]. The effect of active motion on the glass transition has also been previously studied [41,42].

1.3 Micro and macro rheology

1.3.1 Mechanical rheometry

Rheology measures the response of materials to flow and deformation [43]; the rheological properties of gels are important to industrial applications, such as agricultural formulations, foods, paints and coatings, or pharmaceuticals [44–46]. There are many techniques to measure the rheology of materials including: oscillatory rheology, microrheology, atomic force microscopy, or dynamic mechanical analysis, amongst others [43,47].

Mechanical rheology is a widely used technique to characterize the material properties of complex fluids. Rheometers measure stress or strain and convert ratios of the stress and strain to viscoelastic properties, such as the viscosity, storage modulus, or loss modulus [43]. The storage and loss modulus are linear viscoelastic properties determined from the frequency dependent ratio of oscillatory stress to strain [3]. The storage modulus (G'), also called the elastic modulus, measures the energy stored during a strain cycle and describe how solid-like a material is; while the loss modulus (G''), also known as the viscous modulus, measures the energy lost and describes how fluid-like a

material is [3]. The dependence of the viscoelastic moduli (G' and G") on time, frequency, strain, or other variables can describe how materials will flow or deform under certain conditions; which can be useful for design and manufacturing of complex fluids [24,43].

1.3.2 Microrheology

Microrheology is a technique that probes the viscoelastic response of a material based on the microscopic fluctuations of tracer particles embedded within the medium [4,48]. A general approach for microrheology is to quantify the displacements of the probe particle, through particle tracking of microscopy images or scattering experiments, and relate the probe displacements to bulk material properties [3]. Microrheology can be divided into two general categories: passive microrheology, where the motion of the probe particle is governed by diffusion, and active microrheology, where the probe particle is subjected to external forces [48].

For passive microrheology, a generalized Stokes-Einstein relation is used to convert the probe dynamics to the viscoelastic moduli [48]. Equation 6 shows a generalized Stokes-Einstein relation for the complex shear modulus, $G^*(\omega)$, as a function of the mean squared displacement of the probe particle; the complex shear modulus is determined through a Fourier transform of the mean squared displacement [49].

$$G^*(\omega) = \frac{k_B T}{\pi a i \omega \Im\{<x^2(\tau)>\}} \tag{6}$$

Passive microrheology has been shown to accurately describe the mechanical response of materials ranging from aqueous polymer solutions [49] to associating polysaccharides [50] and cross-linked polymer networks [4]. However, instances in which this approach fails or yields an incomplete picture of the rheological response

include active or nonequilibrium materials, anisotropic materials, such as liquid crystals, and materials with large heterogeneities compared to the microscopic probes [3].

1.3.3 Colloidal gel rheology

The mechanical properties of colloidal gels have been extensively studied with mechanical rheology and microrheology. The elastic modulus of colloidal gels scales with the colloid volume fraction [51]; for DLCA fractal gels, the modulus scales as $G \sim \phi_0^{3.5}$, where ϕ_0 is the initial particle volume fraction [52]. The average cluster size, R_c, is also an important parameter in characterizing fractal gel rheology. Krall and Weitz developed a model that estimates the elastic modulus, $G = \kappa_0 a^\beta R_c^{-1-\beta}$, using the average cluster size, spring constant (κ_0), particle radius (a), and elasticity exponent (β) [52]. Microrheological characterizations of fractal cluster gels have suggested that the average cluster size - and not the particle size - is the relevant length scale in the generalized Stokes Einstein equation [53].

1.4 Microstructural engineering for material design

The work presented in this dissertation broadly analyzes the structure and dynamics of materials on the micron scale and the correlations between microscopic and macroscopic material properties. Previous studies of colloidal gels have shown that bulk rheological properties are related to their microscopic structure and dynamics [45,52,54]. The elasticity of colloidal gels arises from the slow dynamics of particles connected in a network structure [52]. Previous research has also shown correlations between the gel microstructure and strain-induced yielding [45]. Because of the connections between microscopic and macroscopic material properties of gels, microstructural engineering is a

valuable approach to formulating industrial applications of colloidal suspensions and gels.

In chapters 2 and 3, we explore the microstructure, dynamics, and rheology of colloidal gels with embedded active matter. Our results demonstrate how active motion can be incorporated into colloidal suspensions as a potential rheology modifier by altering the microscopic dynamics and rheology of the gel network. For industrial applications of colloids, rheology modifiers are used to produce formulations with desired mechanical properties by acting as gelators, thickeners, or emulsifiers [55]. Additives such as associative polymers [56], cellulosic materials [57], and surfactants [58], are incorporated into industrial formulations of colloidal suspensions for applications such as paints and coatings, foods, or consumer products [55,58,59]. The results presented in this dissertation show that active motion could be used as a rheology modifier. We show that incorporating active motion into colloidal gels leads to a decrease in the modulus of the gel network; changes in the gel modulus are correlated with an increase in the microscopic dynamics of the gel network.

Microstructural engineering can also be applied to understand, and potentially control, the macroscopic rheology of polymers. In chapter 4, we explore the relationships between gel stability, rheology, and hydration kinetics of psyllium gels. Psyllium is a polysaccharide that is most commonly used as a dietary fiber supplement; however, its ability to absorb water makes it useful as a gelator or thickener [60,61]. Previous studies have shown a correlation between the microstructure and rheology of psyllium gels [62]; however, less work has examined the microscopic dynamics of these materials.

1.5 Outline of dissertation

This dissertation explores the correlations between microscopic measurements of structure and dynamics to macroscopic mechanical properties of gels. We examine two different types of gels – colloidal gels with embedded active particles and psyllium polysaccharide gels. We use confocal microscopy to image the gels on the microscopic scale and relate our observations on the micron scale to the macroscopic material properties through mechanical rheology.

In chapter 2, we characterize the dynamics of fractal cluster colloidal gels with embedded active colloids. We developed a novel method for incorporating active motion into fractal gels by embedding platinum coated polystyrene Janus colloids into the gel structure and activating the embedded active colloids through controlled delivery of hydrogen peroxide with a hydrogel membrane. We measure the microscopic dynamics of particles in the gel network – both passive and active – and find the addition of active motion into colloidal gels causes an increase in the dynamics of the gel network as measured with the ensemble averaged mean squared displacement. We determine the amount of enhancement in the microscopic dynamics as a function of the total inputted active energy, which is a function of the ratio of active to passive particles and the concentration of hydrogen peroxide. We developed a theory that describes the changes in the gel dynamics that combines direct contributions of the active colloids and indirect contributions, which are modeled using the strain field induced by the displacement of an active colloid embedded in a homogeneous elastic medium.

In chapter 3, we explore rheological implications of embedded active matter in colloidal gels. We developed methods to physically and chemically suppress the

formation of oxygen bubbles formed from the catalytic decomposition of hydrogen peroxide that combine the incorporation of oxygen permeable materials into standard rheometer tooling and the addition of anti-foam chemicals to the gel formulation. Using these techniques, we measured the bulk rheology of gels embedded with active matter. We find the addition of active matter to fractal cluster colloidal gels results in a decrease in the viscoelastic moduli. We characterize the change in the moduli as a function of the total active energy. We compared the viscoelastic moduli obtained from mechanical rheology to values obtained from microrheology through measurements of the microscopic dynamics of the gel. We find that microrheology over-predicts the values of the viscoelastic moduli measured through mechanical rheology. We propose several potential mechanisms for the decrease in the moduli based on the potential changes in the gel structure due to active motion and the effects of active motion acting on the gel to change the dynamics.

In chapter 4, we characterize the kinetics of gelation and hydration of psyllium polysaccharide gels. We analyze the gels formed from three different commercially available psyllium materials with varying grain size – two different powders and husk. Upon mixing with water, psyllium grains absorb water and swell to form a gel. We find that below a certain concentration, the gel phase consolidates and forms a dense sediment enriched in psyllium below polymer depleted aqueous phase. We investigate the role of hydration kinetics on the gel stability and macroscopic rheological properties of psyllium gels. We find the stability of the gel is correlated with gelation kinetics as measured through transient rheological measurements of the viscoelastic moduli and viscosity. We further characterize the hydration kinetics by imaging the psyllium grains with confocal

microscopy during hydration. We use a fluorescent dye that binds with the grains and image the grains during expansion across a wide concentration range and quantify the rate of expansion to extract characteristic timescales for hydration. We do not observe a correlation between timescales of multi-grain hydration kinetics measured through mechanical rheology and the microscopic hydration experiments, which suggest the time to reach plateau viscosity or viscoelastic moduli is related to the expansion of grains.

We conclude this dissertation by summarizing our findings and suggesting future directions to build upon the results presented.

1.6 References

[1]   W. B. Russel, D. A. Saville, and W. R. Schowalter, *Colloidal Dispersions* (Cambridge University Press, 1989).

[2]   P. Romanczuk, M. Bär, W. Ebeling, B. Lindner, and L. Schimansky-Geier, Eur. Phys. J. Spec. Top. **202**, 1 (2012).

[3]   T. M. Squires and T. G. Mason, Annu. Rev. Fluid Mech. **42**, 413 (2010).

[4]   T. A. Waigh, Reports Prog. Phys. **68**, 685 (2005).

[5]   W. F. Paxton, S. Sundararajan, T. E. Mallouk, and A. Sen, Angew. Chemie - Int. Ed. **45**, 5420 (2006).

[6]   W. Wang, W. Duan, S. Ahmed, T. E. Mallouk, and A. Sen, Nano Today **8**, 531 (2013).

[7]   J. Palacci, S. Sacanna, A. P. Steinberg, D. J. Pine, and P. M. Chaikin, Science. **339**, 936 (2013).

[8]   B. M. Mognetti, a. Šarić, S. Angioletti-Uberti, a. Cacciuto, C. Valeriani, and D.

Frenkel, Phys. Rev. Lett. **111**, 1 (2013).

[9] E. J. Hemingway, A. Maitra, S. Banerjee, M. C. Marchetti, S. Ramaswamy, S. M. Fielding, and M. E. Cates, Phys. Rev. Lett. **114**, 1 (2015).

[10] S. J. Ebbens and J. R. Howse, Soft Matter **6**, 726 (2010).

[11] S. Sánchez, L. Soler, and J. Katuri, Angew. Chemie Int. Ed. **54**, 1414 (2015).

[12] S. Wang and N. Wu, Langmuir **30**, 3477 (2014).

[13] J. R. Howse, R. A. L. Jones, A. J. Ryan, T. Gough, R. Vafabakhsh, and R. Golestanian, Phys. Rev. Lett. **99**, 048102 (2007).

[14] S. Ebbens, M. H. Tu, J. R. Howse, and R. Golestanian, Phys. Rev. E - Stat. Nonlinear, Soft Matter Phys. **85**, 1 (2012).

[15] S. C. Takatori, W. Yan, and J. F. Brady, Phys. Rev. Lett. **113**, 028103 (2014).

[16] J. N. Israelachvili, *Intermolecular and Surface Forces*, Third edit (Elsevier Inc., 2011).

[17] R. Van Roij and J. P. Hansen, Phys. Rev. Lett. **79**, 3082 (1997).

[18] J. C. Crocker and D. G. Grier, Phys. Rev. Lett. **73**, 352 (1994).

[19] S. C. Glotzer, Science. **306**, 419 (2004).

[20] G. M. Whitesides and B. Grzybowski, Science. **295**, 2418 (2002).

[21] J. A. Ferrar and M. J. Solomon, Soft Matter **11**, 3599 (2015).

[22] Y. Kim, A. a Shah, and M. J. Solomon, Nat. Commun. **5**, 3676 (2014).

[23] S. Mazoyer, L. Cipelletti, and L. Ramos, Phys. Rev. Lett. **97**, 8 (2006).

[24] P. J. Lu and D. a. Weitz, Annu. Rev. Condens. Matter Phys. **4**, 217 (2013).

[25] C. J. Dibble, M. Kogan, and M. J. Solomon, Phys. Rev. E **74**, 041403 (2006).

[26] V. Prasad, V. Trappe, A. D. Dinsmore, P. N. Segre, L. Cipelletti, and D. A. Weitz,

Faraday Discuss. **123**, 1 (2003).

[27] S. C. Glotzer and M. J. Solomon, Nat. Mater. **6**, 557 (2007).

[28] S. C. Glotzer, Chem. Eng. Sci. **121**, 3 (2015).

[29] A. A. Shah, M. Ganesan, J. Jocz, and M. J. Solomon, ACS Nano **8**, 8095 (2014).

[30] J. A. Ferrar, D. S. Bedi, S. Zhou, P. Zhu, X. Mao, and M. J. Solomon, Soft Matter **14**, 3902 (2018).

[31] X. Mao, Q. Chen, and S. Granick, Nat. Mater. **12**, 217 (2013).

[32] E. Zaccarelli, J. Phys. Condens. Matter **19**, 323101 (2007).

[33] P. J. Lu, E. Zaccarelli, F. Ciulla, A. B. Schofield, F. Sciortino, and D. a Weitz, Nature **453**, 499 (2008).

[34] M. Lattuada, H. Wu, A. Hasmy, and M. Morbidelli, Langmuir **19**, 6312 (2003).

[35] M. Lattuada, H. Wu, and M. Morbidelli, J. Colloid Interface Sci. **268**, 106 (2003).

[36] M. Lattuada, H. Wu, and M. Morbidelli, Chem. Eng. Sci. **59**, 4401 (2004).

[37] N. H. P. Nguyen, D. Klotsa, M. Engel, and S. C. Glotzer, Phys. Rev. Lett. **112**, 075701 (2014).

[38] C. W. Shields and O. D. Velev, Chem **3**, 539 (2017).

[39] S. McCandlish, A. Baskaran, and M. Hagan, Soft Matter **8**, 2527 (2012).

[40] B. van der Meer, L. Filion, and M. Dijkstra, **12**, 3406 (2016).

[41] R. Ni, M. A. Cohen Stuart, M. Dijkstra, and P. G. Bolhuis, Soft Matter **10**, 6609 (2014).

[42] R. Ni, M. A. C. Stuart, and M. Dijkstra, Nat. Commun. **4**, 1 (2013).

[43] H. M. Wyss, Fluids, Colloids Soft Mater. An Introd. to Soft Matter Phys. 149 (2018).

[44] R. Mezzenga, P. Schurtenberger, A. Burbidge, and M. Michel, Nat. Mater. **4**, 729 (2005).

[45] L. C. Hsiao, R. S. Newman, S. C. Glotzer, and M. J. Solomon, Proc. Natl. Acad. Sci. **109**, 16029 (2012).

[46] M. H. Lee and E. M. Furst, Phys. Rev. E **77**, 041408 (2008).

[47] C. J. Macosko, *Rheology: Principles, Measurements, and Applications*, 1st ed. (Wiley-VCH, 1994).

[48]   a M. Puertas and T. Voigtmann, J. Phys. Condens. Matter **26**, 243101 (2014).

[49] B. R. Dasgupta, S.-Y. Tee, J. C. Crocker, B. J. Frisken, and D. A. Weitz, Phys. Rev. E **65**, 051505 (2002).

[50] M. Ganesan, S. Knier, J. G. Younger, and M. J. Solomon, Macromolecules **49**, 8313 (2016).

[51] C. J. Rueb and C. F. Zukoski, J. Rheol. (N. Y. N. Y). **41**, 197 (1997).

[52] A. H. Krall and D. A. Weitz, Phys. Rev. Lett. **80**, 778 (1998).

[53] S. Romer, Aggregation and Gelation of Concentrated Colloidal Suspensions, 2001.

[54] D. Z. Rocklin, L. C. Hsiao, M. Szakasits, M. J. Solomon, and X. Mao, ArXiv Soft Condens. Matter 1 (2018).

[55] R. M. Savage, Food Hydrocoll. **14**, 209 (2000).

[56] A. Page, P. J. Carreau, M. Moan, and M.-C. Heuzey, Can. J. Chem. Eng. **80**, 1181 (2002).

[57] K. Dimic-Misic, P. A. C. Gane, and J. Paltakari, Ind. Eng. Chem. Res. **52**, 16066 (2013).

[58] P. Fernandez, N. Willenbacher, T. Frechen, and A. Kühnle, Colloids Surfaces A

Physicochem. Eng. Asp. **262**, 204 (2005).

[59] C. Karakasyan, S. Lack, F. Brunel, P. Maingault, and D. Hourdet, Biomacromolecules **9**, 2419 (2008).

[60] A. R. Madgulkar, M. R. P. Rao, and D. Warrier, *Characterization of Psyllium (Plantago Ovata) and Its Uses* (Springer, Cham, 2015).

[61] R. Lapasin, *Rheology of Industrial Polysaccharides: Theory and Applications* (Springer US, 1995).

[62] Q. Guo, S. W. Cui, Q. Wang, H. D. Goff, and A. Smith, Food Hydrocoll. **23**, 1542 (2009).

Chapter 2 Dynamics of fractal cluster gels with embedded active colloids

2.1 Abstract

We find that embedded active colloids increase the ensemble-averaged mean squared displacement of particles in otherwise passively fluctuating fractal cluster gels. The enhancement in dynamics occurs by a mechanism in which the active colloids contribute to the average dynamics both directly through their own active motion and indirectly through their excitation of neighboring passive colloids in the fractal network. Fractal cluster gels are synthesized by addition of magnesium chloride to an initially stable suspension of 1.0 μm polystyrene colloids in which a dilute concentration of platinum coated Janus colloids have been dispersed. The Janus colloids are thereby incorporated into the fractal network. We measure the ensemble-averaged mean squared displacement of all colloids in the gel before and after the addition of hydrogen peroxide, a fuel that drives diffusiophoretic motion of the Janus particles. The gel mean squared displacement increases by up to a factor of three for an active to passive particle ratio of 1:20 and inputted active energy – defined based on the hydrogen peroxide's effect on colloid swim speed and run length – that is up to 9.5 times thermal energy, on a per particle basis. We model the enhancement in gel particle dynamics as the sum of a direct contribution from the displacement of the Janus particles themselves and an indirect contribution from the strain field that the active colloids induce in the surrounding passive particles.

2.2 Introduction

Colloidal gels are a class of disordered solids that transition from fluid-like to solid-like behavior as a function of the strength and range of the interparticle attraction and colloid volume fraction. Their slow dynamics arise due to attractive potential interactions that bond particles into a network [1,2]. Diffusion-limited cluster aggregation (DLCA) gels with fractal cluster structure are a well-understood limiting case of disordered gels [1]. Due to the mechanism of aggregation, which corresponds to spinodal decomposition, DLCA gels adopt a fractal cluster microstructure [3]. Investigating the relationships among microstructure, dynamics, and rheology of colloidal gels improves understanding of the relationship between phase equilibrium and dynamical retardation. Furthermore, colloidal gels display finite elasticity at low frequency and a yield stress; controlling these properties is important to industrial applications of gels, including in food, ceramic, pharmaceutical, agricultural, and consumer products [4–6].

Embedding active particles into colloidal gels is a potential route to affect their structure, dynamics, and mechanical properties. At a single-particle level, activity leads to self-propulsion [7], which can be generated by chemical reactions, light, or electric fields [8–10]. Activity can produce crystalline structures through dynamic self-assembly [11,12] or alter equilibrium structures [13,14]. Using active colloids to alter the dynamics of disordered and/or non-ergodic media – such as gels – has received little attention. Activity has been investigated in cross-linked gel networks made with actin filaments, [15,16] a disordered structure. In these materials, ATP-driven molecular motors activate actin, which increases the gel shear modulus [15]. There has been recent

interest in the effect of activity on phase separation [17] and the glass transition [18]. Here we select fractal cluster gels as a model disordered, non-ergodic material to study the effects of introduced active motion.

The structure of fractal cluster gels has been reported to follow

$$g(r) = \frac{c}{a^{d_f}} r^{d_f - 3} \exp(-(\frac{r}{R_c})^\gamma)$$ for r > 4a where $g(r)$ is the radial distribution function, c is a pre-factor set by the density of particles within a cluster, a is the particle radius, d_f is the fractal dimension, R_c is the average cluster size, and γ is the cut-off exponent [19]. For r < 4a, short-range effects leads to specimen specific, non-fractal scaling [19]. The average cluster size, R_c, is $R_c = a\phi_0^{d_f - 3}$, where ϕ_0 is the particle volume fraction. A fractal dimension d_f=1.8 is typical for DLCA gels. The low-frequency elastic modulus is $G_0 = \kappa_0 a^\beta R_c^{-1-\beta}$, where κ_0 is the bond stiffness and β is the elasticity exponent [20]. The microscale dynamics of particles in passive fractal cluster gels is related to their elastic modulus by $\lim_{t \to \infty} <x^2(t)> = \frac{k_b T}{\pi R_c G_0}$, where $<x^2(t)>$ is the ensemble-averaged mean squared displacement of particles within the gel. The dynamics of particles within the (passive) gel network are inversely proportional to the elasticity.

Here we show that the dynamics of a gel particle network are significantly affected when active motion is imparted to a dilute fraction of colloids. We embed Janus particles that are activated by hydrogen peroxide into fractal cluster gels and find that the mobility of the gel network increases with the additional Janus particle activity. This increase is generated by the sum of a direct contribution of the active particles to the gel

dynamics and an indirect contribution in which the active particles enhance dynamics of surrounding passive particles due to their mutual connectivity in the fractal cluster network.

2.3 Materials and methods

2.3.1 Synthesis of Janus colloids and fractal gels

Fractal cluster gels are produced from 1.0 ± 0.03 μm diameter carboxylate modified polystyrene microspheres (Nile red fluorescent, #F8819 ThermoFisher Scientific). Janus particles are synthesized by spin coating (300 rpm for 20 seconds and 3000 rpm for 40 seconds) these spheres onto a cleaned glass side. 20 nm of platinum is deposited on the exposed surface of the spheres by physical vapor deposition (Enerjet electron beam evaporator, deposition rate 1 Å/s). Janus particles were removed from slides, sonicated, and washed three times in DI water [21]. The Janus features of the particles were confirmed by scanning electron microscopy. To allow 3D confocal microscopy visualization as needed, the solvent used is a photo-polymerizable aqueous solution consisting of 67 wt. % water, 33 wt. % poly(ethylene glycol) diacrylate (MW 750), and 0.03 g/mL lithium-phenyl-2,4,6-trimethylbenzoylphosphinate (TMPPL) photoinitiator [5,22]. The viscosity of this solution is 4.5×10^{-3} Pa·s.

2.3.2 Delivering activity to fractal gels

The hydrogel membrane that is used to deliver H_2O_2, is synthesized through photopolymerization of 33.2 wt. % poly(ethylene glycol) diacrylate (MW 750), 66.4 wt. % water, and 0.4 wt. % photoinitiator 2-hydroxy-2-methyl-propiophenone [23]. Delivering H_2O_2 through the membrane allows the chemical to diffuse slowly into the gel

without generating any flow that might disrupt the gel network, which is itself weak (estimated $G_0 \sim 0.01$ Pa [20]). This method to deliver H_2O_2 ensures that changes to the gel network are due solely to active motion, rather than any effect of mixing. A schematic and image of the device are shown in Figure 1C and 1D. The volume of the colloidal gel sample enclosed within the membrane is 200 μL. We add 400 μL of aqueous hydrogen peroxide solution (0-12 wt.%) outside of the membrane. To calculate the concentration of H_2O_2 in the gel sample, we assume equimolar counterdiffusion. Therefore, the added H_2O_2 is diluted to a final volume of 600 μL, which corresponds to a concentration of 0-8 wt. % H_2O_2 within the colloidal gel sample.

2.3.3 Visualization and image analysis of colloidal gel structure and dynamics

2D time series images of the gels were taken one hour after salt was added to induce gelation. We take a 60 s series of images at a frame rate of 15 frames per second in five pre-defined locations 10 microns above the coverslip spaced 100 microns apart, with a pixel size of 83 nm/pix. 30 minutes after the addition of H_2O_2, we capture another 60 s series of images in the same manner. To analyze 3D gel volumes, we use a python implementation of a watershed image analysis algorithm [24]. To analyze 2D time series images, we use trackpy [25], a python implementation of a local brightness maximum image analysis algorithm [26], to determine the positions of particles and compute the mean squared displacement of all particles in the gel. Particles are resolved to ± 15 nm in the image plane, as determined by measurement of the static error [27]. Trajectories in Figure 4a-c are produced using Mosaic, a particle tracking plugin for Fiji [28,29].

2.4 Results

The mean squared displacement (MSD) of particles in a gel network with embedded Janus particles increases after the Janus particles are activated by H_2O_2. This enhancement is apparent by comparing the trajectories of particles in Fig. 4c (from indicated region of interest (ROI) in passive gel, Fig 4a) and Fig. 4d,e (from ROIs in active gel, Fig 4b.). These data were acquired at a fixed active to passive colloid ratio of 0.05 with 6.7% H_2O_2. Figure 4d and 4e show that the displacement of the particular particles identified in the two ROI are aligned in a direction parallel to the orientation of the local colloidal cluster or filament; however, a more general analysis of N = 78 particles in different clusters finds that the particle dynamics tend to be aligned perpendicular to the local cluster orientation, Figure 5. When the dynamics of all particles are averaged, the MSD is isotropic, because the fractal cluster structure itself is isotropic.

We compute the ensemble-averaged MSD before and after the addition of H_2O_2, shown in Figure 4f, and find a significant increase in the MSD after H_2O_2 addition. Gels – both before and after H_2O_2 addition – display MSD curves that are nearly independent of time, with $<x^2(t)>$ increasing as a power law with a small exponent of ~ 0.15; this behavior is consistent with prior literature [30] and indicates nearly all colloids - active and passive - are localized within the gel network and the role of large-scale structural rearrangements is weak. Deviations from the ideal plateau dynamics could have multiple origins, including slow syneresis [31], arrested phase separation [32], or thermal expansion [33].

A kinetic study showed that the gels slowly age over the period of the measurements (Figure 6) and in Figure 4f there is delay of 30 minutes between

measurement of the passive gel dynamics and the active gel dynamics, to allow H_2O_2 diffusion. However, the change in gel MSD due to aging over a comparable 30-minute period is never more than 20%, which is much less than the change in dynamics due to H_2O_2 addition. The results of Figure 4f can also be compared to the control experiment in which the same concentration of H_2O_2 is delivered to a gel comprised of just passive particles. In this case, the average MSD drops by the small percentage of ~ 30%. Evidently, the H_2O_2 – a strong oxidizer – modulates the bond strength of passive particles in the gel to a small degree, in addition to its role in active motion. This effect was found to be, within error, independent of concentration (Fig 7) and in the opposite direction of the change when active particles were present. To account for this and plot only the effect of active motion, we report a measure $\delta(\tau)$ of the enhanced dynamics due to activity, computed as:

$$\delta(\tau) = \frac{<x^2(\tau)>_{H_2O_2,Janus} <x^2(\tau)>_{NoH_2O_2,Passive}}{<x^2(\tau)>_{NoH_2O_2,Janus} <x^2(\tau)>_{H_2O_2,Passive}}$$

(1)

The MSD enhancement, $\delta(\tau)$, describes the ratio of the ensemble averaged MSD of the active and passive gels, corrected by the effect that adding H_2O_2 has on the passive gel.

$\delta(\tau)$ increases with increasing H_2O_2 concentration at a fixed active to passive particle ratio of 0.05 (Fig 9a). The enhancement is approximately independent of time and increases linearly as a function of the H_2O_2 concentration, Figure 9b. By embedding 5% active particles within the gel, the dynamics of all particles – both passive and active together – are enhanced by up to a factor of three. Both the number of active colloids and the H_2O_2 concentration affect activity. Varying the ratio of active to passive colloids from 1:20 to 1:8 (Figure 9c) increases $\delta(\tau)$. By increasing the number of active particles

24

within the gel, we observe an increase in the gel mobility of up to about four times greater than passive gels.

While passive gel dynamics are driven by thermal energy, active gels are driven by energy inputted into the system by the catalytic oxidation of H_2O_2. Following Takatori et al, the active energy of a particle, E_A, is given by ξVl, where ξ is the hydrodynamic drag coefficient, V is the active particle's run velocity in free solution, and l is the active particle run length, equivalent to $l = \tau_R V$ where τ_R is the Brownian reorientation time, $\tau_R = \dfrac{8\pi\mu a^3}{k_B T}$ [34]. The free particle velocity is determined by fitting the MSD of the active colloids at each H_2O_2 concentration to $\Delta x^2 = 4D\Delta t + V^2 \Delta t^2$, the limiting form of the active particle MSD at short times [7]. Results for each H_2O_2 concentration are in Table A-1. Over the range of H_2O_2 concentrations studied, the activity imparted generates energies on a per particle basis that are 4.5 - 9.4 times greater than thermal energy. The ratio of active to passive energy in the gel is then:

$\dfrac{X_{active} E_{active}}{X_{passive} E_{passive}} = \dfrac{X_{active} \xi V \tau_R}{X_{passive} k_B T}$. Using this scaling, the effects of active particle number and

H_2O_2 concentration collapse onto one curve, Fig. 9d.

We present a simple model for the enhancement in gel dynamics induced by the embedded active particles. The model resolves the active particle's effect into direct and indirect contributions. Each active particle directly contributes a relative enhancement of

$\dfrac{E_{active}}{k_B T}$ to the gel dynamics. The active particles also contribute indirectly to the MSD enhancement by inducing a strain field on the surrounding passive particles in the fractal

cluster, which is the response of the surrounding passive particles to the active motion. This indirect contribution is modeled by assuming that the fractal cluster gel is a linearly elastic medium. The deformation field, $\mathbf{u}(\mathbf{x})$, induced by the displacement of the active particle in the gel is:

$$\mathbf{u}(\mathbf{x}) = \frac{3a}{10-12v}\left[\left(\frac{3-4v}{r}+\frac{a^2}{3r^3}\right)\mathbf{U}+\left(1-\frac{a^2}{r^2}\right)\frac{\mathbf{U}\cdot\mathbf{xx}}{r^3}\right]$$

(2)

where r is the radial distance, v is the Poisson ratio, a is the particle radius, $\mathbf{U}$ is the active particle displacement, and $\mathbf{x}$ is the particle position [6]. This induced strain field, plotted in Figure 4a, is anisotropic and long range. We use a value of $v = 0.5$ and show effects of varying v in A- 2.

The predicted direct contribution of the active particles to the MSD can be compared to measurements of the localization of Janus particles in the gel by reflection CLSM of the platinum layers (Fig 2c). We compute $\delta(\tau)$ for the embedded Janus particles with 6.7% H_2O_2. At long times, $\delta(\tau) \sim 7$, the enhancement is significantly greater than for the passive particles, $\delta_{passive} \sim 2.5$, and comparable to the active energy, $\frac{E_{Active}}{k_B T} = 9.0$ predicted from single-particle measurements (Figure 10b and Table A-1).

By summing the passive, direct, and indirect contributions, the MSD enhancement of the active gel is:

$$\delta(t) = 1 + X_{active}\left\{\frac{E_{active}}{k_B T}+X_{passive}\int_{2a}^{R_c}4\pi r^2\,dr\int_0^{\pi}\sin\theta\,d\theta\int_0^{2\pi}g(r)<u(r,\theta,\phi)^2>d\phi\right\}$$

(3)

The first term (unity) accounts for the passive motion. The second term includes the two effects of activity – the direct and indirect contributions. The indirect contribution from the induced strain field is calculated by integrating over the anisotropic strain field (eqn 2) induced in a gel with an isotropic fractal structure given by $g(r)$. We use the experimentally measured g(r) for r <4a and the fractal cluster model for r > 4a [19] (c.f. Appendix A-1). We compute the MSD enhancement from the direct (δ_{direct}) and indirect ($\delta_{indirect}$) contributions, plotted in 10c inset. The integration of the right hand term is carried out to the cluster radius, consistent with other microrheology models of fractal gels [20,35]; however, the particular choice of R_c is not critical, because g(r) is low for r > R_c (c.f. Supporting Information).

Although smaller than the direct contribution, the indirect contribution to the active gel MSD is still significant (c.f. Figure 4c). The theory underpredicts the MSD enhancement, particularly at high H_2O_2 concentrations. Reasons for the model underestimation might be: (i) non-ideal experimental conditions, such as an inhomogeneous concentration of Janus particles in the gel; (ii) interactions among the strain-fields induced by neighboring Janus particles; (iii) reflections of induced deformations of surrounding passive particles back onto the active particle excitation; (iv) deviations of the fractal cluster structure elastic response from that of a homogeneous elastic medium; (v) the model's inclusion of only intra-cluster effects, consistent with the strong-link regime of fractal cluster models [20,35]. Future work addressing points (iv) and (v) could yield a higher fidelity description of the strain field induced by active Janus particles in the fractal cluster gel.

Active particles embedded within a fractal gel network increase the average mobility of particles in the gel. The amount of dynamical enhancement collapses onto a single curve when the energy that an active particle contributes to the gel is determined by the swim pressure [34]. $\delta(\tau)$ increases linearly with $\dfrac{N_A E_A}{N_B E_B}$ over the parameter range studied; $\delta(\tau)$ is predicted with some underestimation when direct and indirect contributions of the active particles to the gel dynamics are modeled. Here we focused on the microdynamical changes induced in a gel with embedded activity; having found they are significant, future work might analyze how the activity affects other microdynamical changes, such as the correlated 2D displacement field generated around an active particle by its fluctuations and the macroscopic rheological properties of the elastic fractal cluster gel. Effects which could be observable include a change in the gel elastic modulus, as well as swelling of the gel induced by the active particles embedded within it [36].

2.5 Acknowledgments
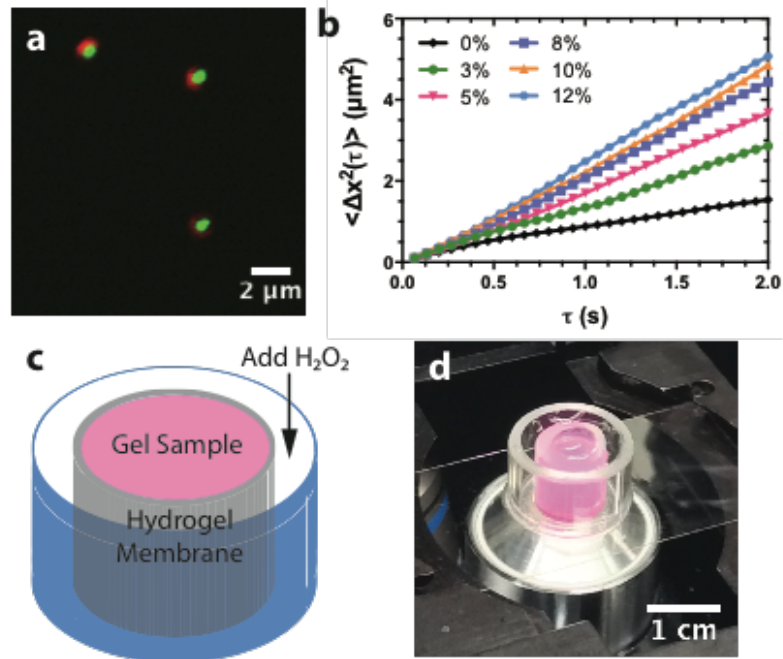
Figure 2-1. Experimental methods for delivering activity to colloidal gels. A) Confocal laser scanning microscopy image of produced Janus particles. B) Free particle mean squared displacement of Janus particles activated by hydrogen peroxide. C) Schematic and D) image of experimental set-up.
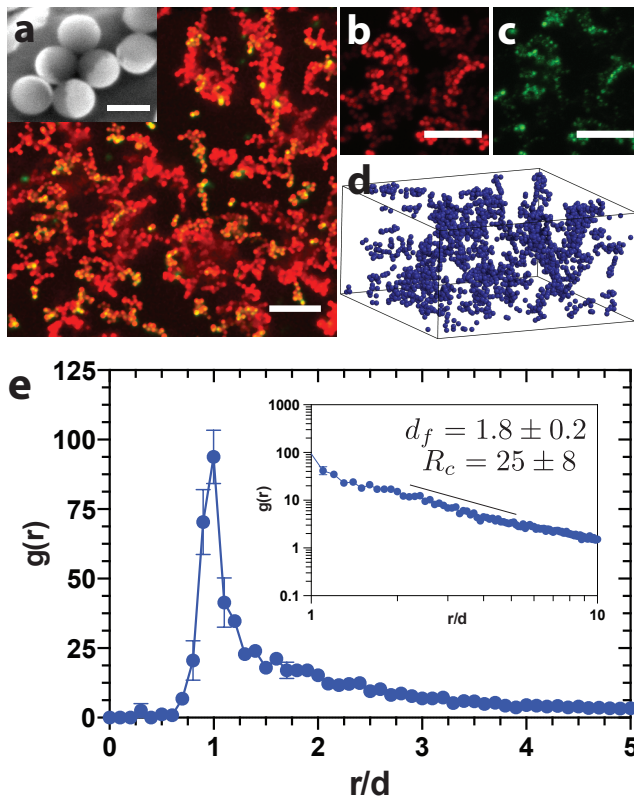
Figure 2-2. Visualization and characterization of gel 3D structure. A) 3D projection of fractal cluster gel embedded with Janus particles with scanning electron microscopy image inset (scale bar 1 μm), B) fluorescent and C) reflective channels, scale bar A-C) 10 μm. D) Rendering of gel produced from 3D image analysis. E) Radial distribution function with fractal dimension and average cluster size inset.
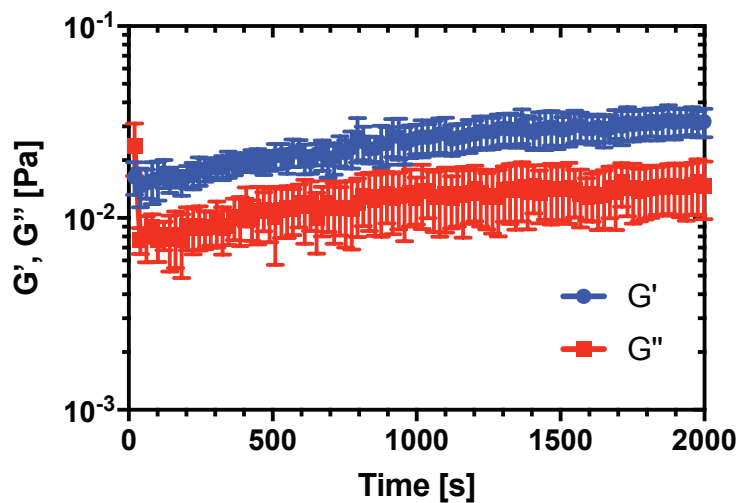
Figure 2-3. Time dependent rheology of passive gel network measured on ARG2 rheometer with 60 mm parallel plate fixture, 300 μm gap, 0.1 Hz frequency, and 0.001 strain. The experimentally measured elastic modulus reaches a steady state value of 0.03 ± 0.01 Pa after 1500 s.
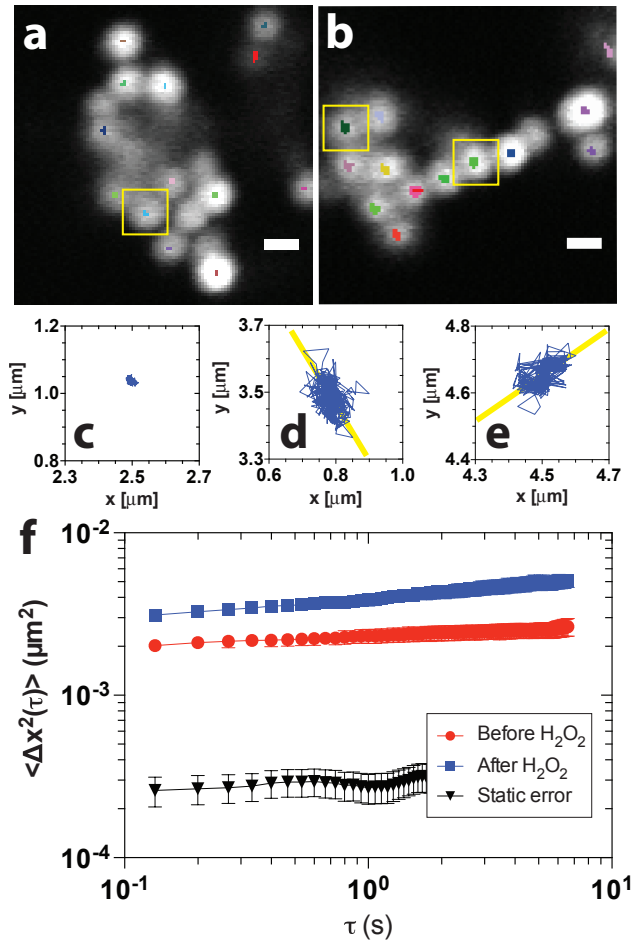
Figure 2-4. Single particle and ensemble averaged active gel dynamics. A) Trajectory of passive gel. B) Trajectory of active gel. C) Single particle dynamics of a passive gel trajectory. D-E) Single particle dynamics in two active gel trajectories, with local orientation of cluster plotted as an overlaid line. F) Ensemble averaged MSD of gel before and after addition of 6.7% hydrogen peroxide.
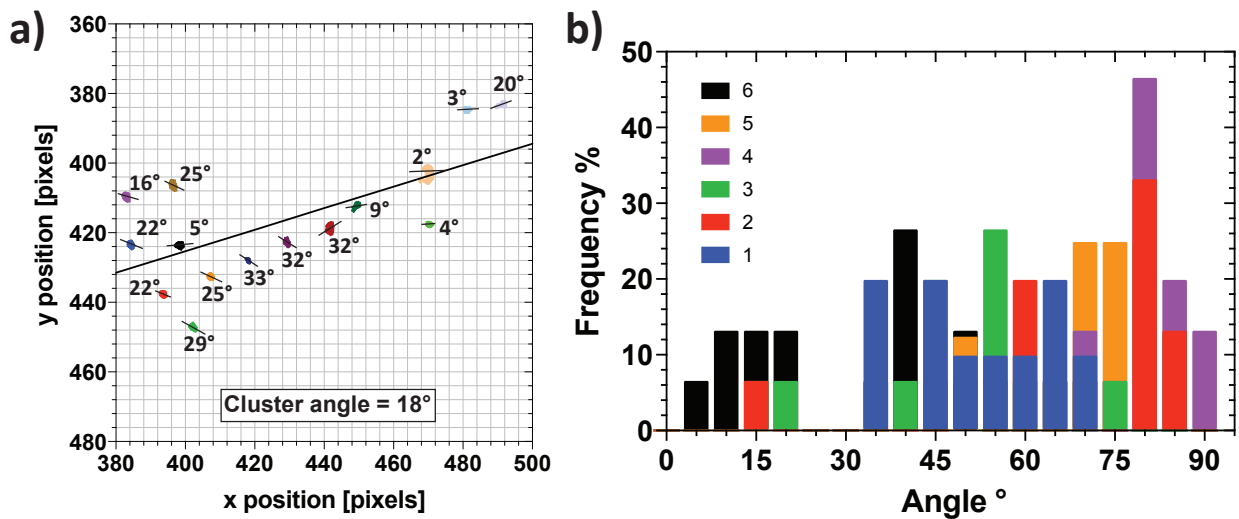
Figure 2-5. Determining the angle between the local cluster orientation and the dynamics of particles in the local cluster. a) The orientation of one cluster is determined by fitting a line to all particle positions in the cluster. The average orientation of each particle in the cluster was determined by fitting a line to the particle positions over time. The angle of the trajectory for each particle is indicated by a line and angle. Angles are relative to the x-axis of the image b) We analyzed all particles within a cluster for six different clusters and plotted the probability distribution for the angle between the cluster and trajectory. Because most of the measured angles are preferentially located in the range 45-90°, rather than the range 0-45°, we conclude that the particles in a cluster tend to move perpendicularly to the orientation of that cluster.
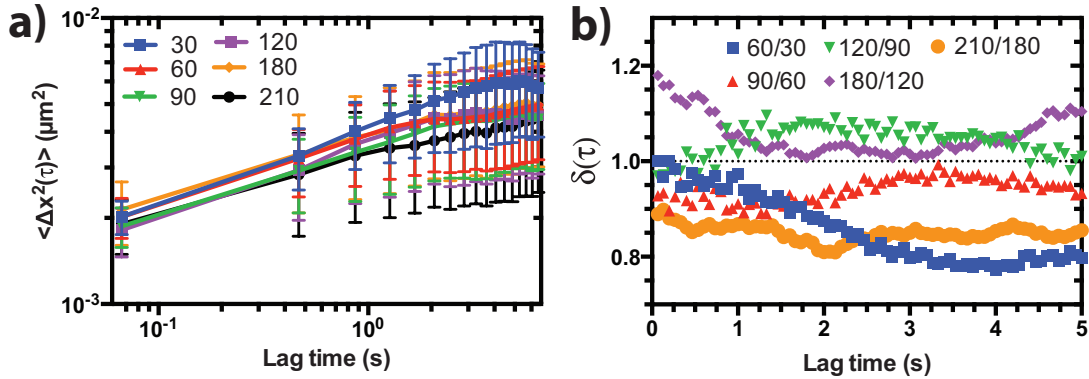
Figure 2-6. Gelation kinetics and aging of passive gels. a) Mean squared displacement of the passive gel measured 30-210 minutes after preparation of the gel. Gel aging is apparent. b) $\delta(t)$ values calculated for changes in time at 30 minute intervals; the notation is that 60/30 indicates the ratio of the passive gel mean squared displacements at 60 minutes over the passive gel mean squared displacement measured at 30 minutes, $<x^2(60)>/<x^2(30)>$, based on the data from Figure 6a. The different data sets in Figure 6b are all separated by 30 minutes to allow comparison to the effect of adding activity, which also requires a 30 minute delay. The values of $\delta(t)$ reported in Figure 6b can be compared to those in Figure 9, which were done from 60-90 minutes after preparation of the gel, and with a 30 minute delay between measurement of the passive and active mean squared displacements. Figure 6b shows there is less than a 20% change in gel particle dynamics over 30 minute intervals due to aging. This 20% change is much smaller than the up to factor of three increase mean squared displacement due to added activity reported in the main text.
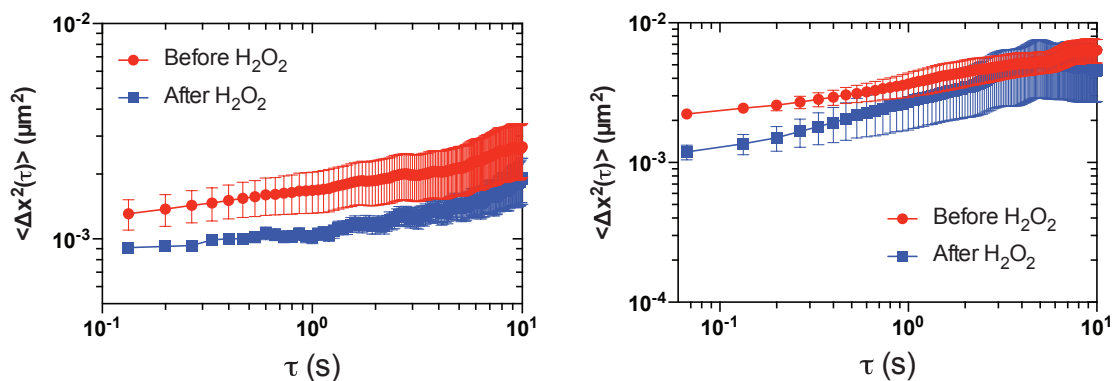
Figure 2-7. Stiffening of passive gels from H_2O_2. Mean squared displacement (MSD) before and after addition of left) 3.3% and right) 6.7 % H_2O_2 to a passive gel with no embedded Janus particles. We find the average MSD drops by a small percentage, and this effect is, within error, independent of the two H_2O_2 concentrations studied.
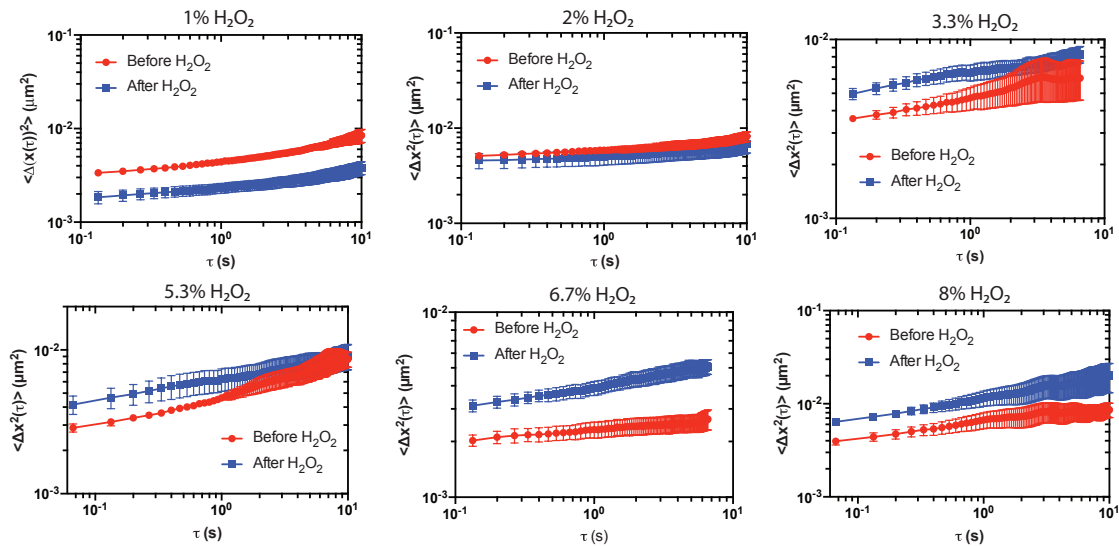
Figure 2-8. Mean squared displacement (MSD) before and after addition of 1 - 8 w/v% H_2O_2 at a fixed active to passive particle ratio 0.05. At low activity (1-2% H_2O_2), there is a decrease in the gel MSD due to the H_2O_2 stiffening the gel network. At concentrations of 3.3% H_2O_2 and higher, the active particles provide enough energy to increase the gel MSD. The enhanced dynamics of the active gels increases with increasing H_2O_2 concentrations.
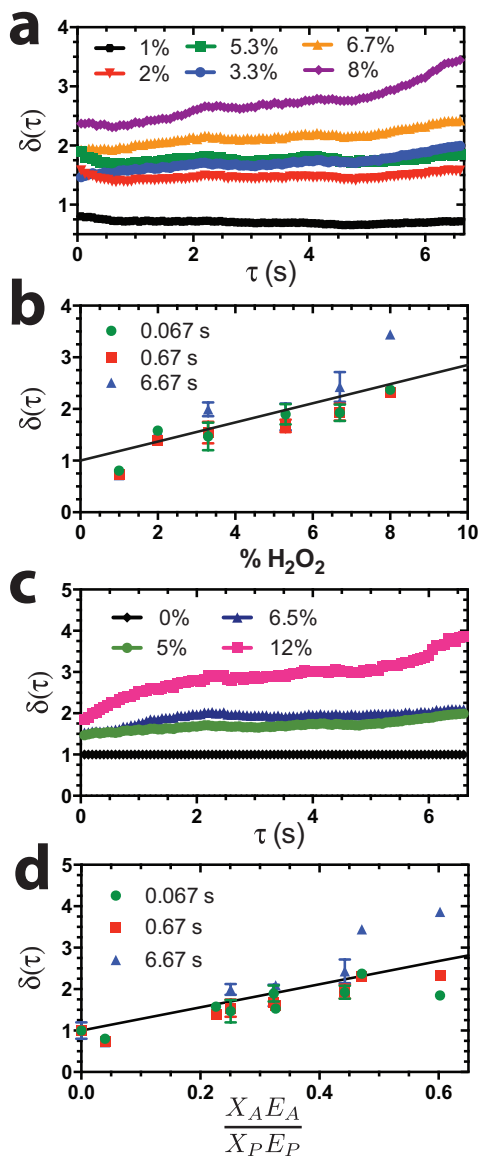
Figure 2-9. Active gel ensemble averaged dynamics. A) MSD enhancement at a fixed active to passive particle ratio of 0.05 varying the hydrogen peroxide concentration. B) $\delta(\tau)$ values at lag times 0.067, 0.67, and 6.67 s as a function of the hydrogen peroxide concentration at a fixed active to passive particle ratio of 0.05. C) MSD enhancement at a fixed hydrogen peroxide concentration of 3.3% varying the ratio of active to passive particles. D) $\delta(\tau)$ values at lag times 0.067, 0.67, and 6.67 s at each hydrogen peroxide and active particle concentration.
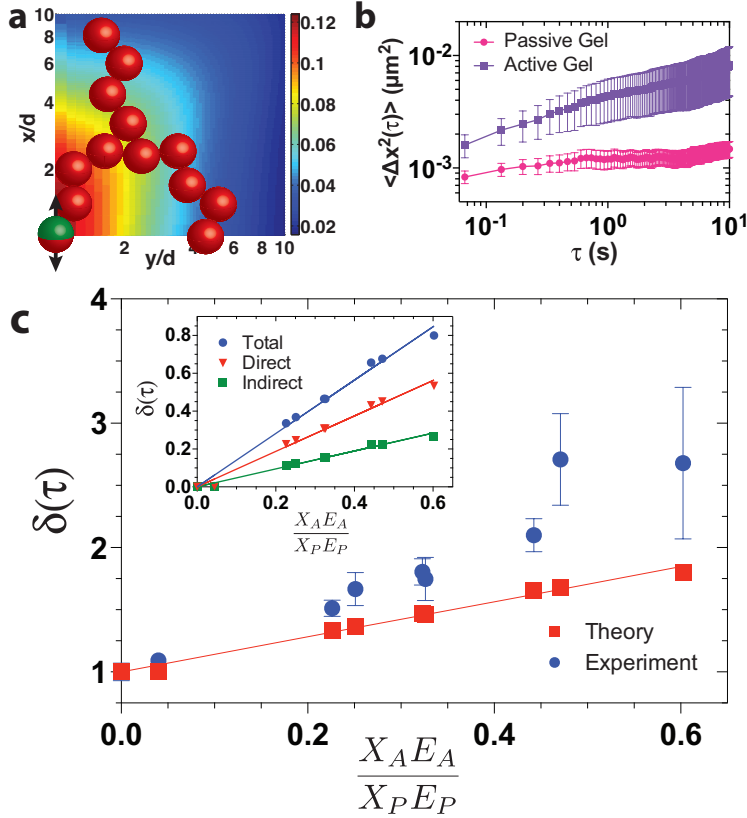
Figure 2-10. Origin of the global enhancement in gel particle dynamics. A) Strain field induced on gel network by displacement of active particle for active to passive particle ratio 0.05 and 6.7% H_2O_2, where U_x is 0.2 μm. Color bar shows magnitude of the strain field in microns. B) MSD of Janus particle in gel network before and after addition of 6.7 % H_2O_2. C) Comparison of experimental MSD enhancement to predicted values, with total enhancement, direct and indirect contributions inset. Theory values were calculated point-wise at each experimental condition using parameters measured for free active particles. Lines for theory are to guide the eye.

2.6 References

[1]   V. Prasad, V. Trappe, A. D. Dinsmore, P. N. Segre, L. Cipelletti, and D. A. Weitz, Faraday Discuss. **123**, 1 (2003).

[2]   E. Zaccarelli, J. Phys. Condens. Matter **19**, 323101 (2007).

[3]   M. Carpineti and M. Giglio, Phys. Rev. Lett. **68**, 3327 (1992).

[4]   R. Mezzenga, P. Schurtenberger, A. Burbidge, and M. Michel, Nat. Mater. **4**, 729 (2005).

[5]   L. C. Hsiao, R. S. Newman, S. C. Glotzer, and M. J. Solomon, Proc. Natl. Acad. Sci. **109**, 16029 (2012).

[6]   M. H. Lee and E. M. Furst, Phys. Rev. E **77**, 41408 (2008).

[7]   J. R. Howse, R. A. L. Jones, A. J. Ryan, T. Gough, R. Vafabakhsh, and R. Golestanian, Phys. Rev. Lett. **99**, 48102 (2007).

[8]   S. Sánchez, L. Soler, and J. Katuri, Angew. Chemie Int. Ed. **54**, 1414 (2015).

[9]   S. J. Ebbens and J. R. Howse, Soft Matter **6**, 726 (2010).

[10] W. F. Paxton, S. Sundararajan, T. E. Mallouk, and A. Sen, Angew. Chemie - Int. Ed. **45**, 5420 (2006).

[11] J. Palacci, S. Sacanna, A. P. Steinberg, D. J. Pine, and P. M. Chaikin, Science. **339**, 936 (2013).

[12] N. H. P. Nguyen, D. Klotsa, M. Engel, and S. C. Glotzer, Phys. Rev. Lett. **112**, 75701 (2014).

[13] S. McCandlish, A. Baskaran, and M. Hagan, Soft Matter **8**, 2527 (2012).

[14] B. van der Meer, L. Filion, and M. Dijkstra, **12**, 3406 (2016).

[15] T. B. Liverpool, M. C. Marchetti, J.-F. Joanny, and J. Prost, Europhys. Lett. **85**,

18007 (2009).

[16] D. Mizuno, C. Tardin, C. F. Schmidt, and F. C. MacKintosh, Science. **315**, 370 (2007).

[17] I. Buttinoni, J. Bialké, F. Kümmel, H. Löwen, C. Bechinger, and T. Speck, Phys. Rev. Lett. **110**, 238301 (2013).

[18] A. Yazdi and M. Sperl, Phys. Rev. E **94**, 32602 (2016).

[19] M. Lattuada, H. Wu, and M. Morbidelli, J. Colloid Interface Sci. **268**, 106 (2003).

[20] A. H. Krall and D. A. Weitz, Phys. Rev. Lett. **80**, 778 (1998).

[21] A. A. Shah, B. Schultz, K. L. Kohlstedt, S. C. Glotzer, and M. J. Solomon, Langmuir **29**, 4688 (2013).

[22] T. Majima, W. Schnabel, and W. Weber, Die Makromol. Chemie **192**, 2307 (1991).

[23] J. Scrimgeour, J. K. Cho, V. Breedveld, and J. Curtis, Soft Matter **7**, 4762 (2011).

[24] L. C. Hsiao, B. A. Schultz, J. Glaser, M. Engel, M. E. Szakasits, S. C. Glotzer, and M. J. Solomon, Nat. Commun. **6**, 8507 (2015).

[25] D. Allan, L. Uieda, F. Boulogne, R. W. Perry, T. A. Caswell, and N. Keim, (2014).

[26] J. Crocker and D. Grier, J. Colloid Interface Sci. **310**, 298 (1996).

[27] T. Savin and P. S. Doyle, Biophys. J. **88**, 623 (2005).

[28] J. Schindelin, I. Arganda-Carreras, E. Frise, V. Kaynig, M. Longair, T. Pietzsch, S. Preibisch, C. Rueden, S. Saalfeld, B. Schmid, J.-Y. Tinevez, D. J. White, V. Hartenstein, K. Eliceiri, P. Tomancak, and A. Cardona, Nat. Methods **9**, 676 (2012).

[29] Y. Gong, Thesis 243 (2015).

[30] C. J. Dibble, M. Kogan, and M. J. Solomon, Phys. Rev. E **74**, 41403 (2006).

[31] L. Cipelletti, S. Manley, R. C. Ball, and D. A. Weitz, Phys. Rev. Lett. **84**, 2275 (2000).

[32] P. J. Lu, E. Zaccarelli, F. Ciulla, A. B. Schofield, F. Sciortino, and D. a Weitz, Nature **453**, 499 (2008).

[33] S. Mazoyer, L. Cipelletti, and L. Ramos, Phys. Rev. Lett. **97**, 8 (2006).

[34] S. C. Takatori, W. Yan, and J. F. Brady, Phys. Rev. Lett. **113**, 28103 (2014).

[35] W.-H. Shih, W. Y. Shih, S.-I. Kim, J. Liu, and I. A. Aksay, Phys. Rev. A **42**, 4772 (1990).

[36] S. C. Takatori and J. F. Brady, Soft Matter **10**, 9433 (2014).

Chapter 3 Rheological implications of embedded active matter in fractal cluster gels of colloidal particles

3.1 Abstract

We find that dilute concentrations of embedded active colloids decrease the linear viscoelastic moduli of fractal cluster colloidal gels. The motivation for this work is potential tuning of colloidal gel rheology through control of the microscopic dynamics of embedded active particles. The majority of the particles in the gel are polystyrene colloids aggregated into well-known fractal cluster gels by addition of divalent electrolyte. The embedded active particles are Janus particles with a catalytically active platinum hemisphere. Upon addition of hydrogen peroxide – a fuel that drives the diffusiophoretic motion of the colloids – the microdynamics and mechanical rheology change with the concentration of hydrogen peroxide and the number of active colloids. The measured decreases in the elastic and viscous moduli are correlated with an increase in the microdynamics of the gel network; the degree of enhancement is a function of the active energy of the Janus colloids. We examine hypotheses that might explain the degree of rheological change generated by the embedded active matter; the decrease in the modulus is likely caused by the active motion inducing changes on the dynamics of the gel network. Control of the mechanical properties of colloidal gels – as made possible by the findings presented here – can potentially be used to tune the mechanical properties of materials such as paints and coatings, pharmaceuticals, and agricultural formulations.

3.2 Introduction

Active matter is ubiquitous in nature; examples include the flocking of birds, the swarming of bacteria, or the contraction of actin filaments in the cytoskeleton [1–3]. There has been recent interest in developing synthetic active particle systems on the nano and colloidal scale for applications such as drug delivery, sensors, or soft robotics [4,5]. At a single particle level, active motion leads to self-propulsion of the particle [6]. There are several mechanisms for generating active motion, such as light, electric fields, or chemical potential gradients [4,5,7]. A frequently used active particle system is the self-diffusiophoretic transport of platinum coated Janus colloids that are activated by hydrogen peroxide [6]. Platinum catalyzes the decomposition of hydrogen peroxide (H_2O_2) into H_2O and O_2; the decomposition generates a concentration gradient around the particle because of the Janus feature. This concentration gradient leads to self-propulsion.

When used in self-assembly, active motion can create dynamic and reconfigurable structures that are inaccessible in purely Brownian suspensions. Active motion has been used to make living crystals comprised of dynamic aggregates that can be manipulated through light and magnetic fields [1,2]. Combining particle anisotropy with active motion leads to more complex assemblies such as the rotating crystalline phases formed from rotating gear-like particles [8]. Furthermore, mixtures of active and passive particles have produced phenomena such as coherent clustering and the formation of transient lanes [9]. Active motion can also be used to alter the equilibrium structures formed by passive particles. For example, it can enhance crystallinity by increasing the mobility of particles at the grain boundaries, which promotes annealing [10].

Less work has focused on the effects of active motion on the mechanical properties of colloidal suspensions. Most research on the rheology of active systems has focused on actin gels that are activated by myosin motors and adenosine triphosphate (ATP) [11,12]. In these systems, the addition of activity, through myosin and ATP, leads to an increase in the modulus of the gel network. The explanation for the observed behavior is that myosin motors apply an internal, isotropic stress (i.e. tension) to the actin network. This internal tension causes the actin network it to become more rigid [11]. The mechanical response of active bacterial suspensions has also been studied [3,13,14]. Adding a small fraction of active bacteria ($\phi \sim 10^{-3}$) to water caused no change in the solution viscosity in spite of super-diffusive behavior of the bacteria, as characterized through one and two-point microrheology [14]. However, measurements of higher concentrations of bacteria have shown a decrease in viscosity due to activity [13].

Activity is a promising method to alter the rheology of colloidal assemblies or to create materials with dynamic or reconfigurable mechanical properties. Here, we investigate the effects of active motion on the rheology of colloidal gels. Colloidal gels are a state of soft matter characterized by attractively bonded particles immobilized in a network [15,16]. Gels have interesting rheological properties, such as linear elasticity and a yield stress [17,18]. Controlling these properties is important to industrial applications of gels including their use in food, paints and coatings, as well as in pharmaceutical products and agricultural formulations [17,19,20]. The specific type of colloidal gel we study here are fractal cluster gels, produced by slow aggregation of dilute concentrations of polystyrene latex. These gels are good approximation of commercial materials; well-

tested theory that relates gel microstructure, dynamics, and macroscopic rheology is available for fractal cluster gels [16,21,22].

Active particles embedded within colloidal gels could allow for the creation of gels with multi-state mechanical properties through addition and depletion of the active component. Previous research has shown that active particles embedded within colloidal gels increase the microscopic dynamics of the gel network. [23] At least for a fully passive (Brownian) system, such an increase in dynamics would induce a decrease in the elastic modulus of the gel [21]. This connection arises because the mean squared displacement of particles in the gel is related to its modulus through a generalized Stokes-Einstein equation. However, the use of this equation to relate dynamics to mechanical properties requires that the system obey the fluctuation-dissipation theorem, which assumes the energy imparted on a particle through Brownian fluctuations is dissipated through viscous drag forces [24]. Because active motion is out of equilibrium, there is no expectation that colloidal gels with active colloids obey the fluctuation dissipation theorem; in fact, violations of the fluctuation dissipation theory have been previously reported in active actin gels [11].

In this work, we introduce active motion into colloidal gels and explore how activity affects the rheology of the gel network. We characterize the microdynamics and rheology of passive gels (comprised fully of Brownian particles) and active gels (comprised principally of Brownian particles with a small fraction of embedded active Janus colloids). We find the addition of active motion leads to a decrease in both the elastic and viscous modulus of the gel. We characterize the change in the modulus as a function of the active energy input, which is controlled by the ratio of active to passive

particles and the concentration of hydrogen peroxide. We further explore the connection between the microscopic dynamics and rheology of the active gels through comparison of the frequency dependent moduli obtained by particle tracking and microrheology and by direct, macroscopic rheological measurements.

3.3 Materials and Methods

Preparation of colloidal gels

Gels were self-assembled by addition of 64 mM $MgCl_2$, a divalent salt that induces slow aggregation, to an initially stable suspension of Janus and polystyrene colloids (1.0 ± 0.031 μm carboxylate modified polystyrene microspheres, purchased from Thermo Fisher Scientific). Janus particles were synthesized by spin coating the polystyrene colloids onto cleaned glass slides and depositing a 10 nm platinum layer on one side of the particle through physical vapor deposition [25]. Particles were removed from the slide and washed with DI water three times. Gels were suspended in a density-matched solvent of D_2O and H_2O. Janus colloids were activated by hydrogen peroxide (H_2O_2), which was added at the time of formulation. An anti-foam chemical (Xiameter 1410, Dow Chemical) was used to suppress formation of oxygen bubbles from decomposition of H_2O_2 [26,27]. The imaging device was an 8 well chamber slide (purchased from Thermo Fisher Scientific).

The activity of the Janus colloids was characterized by direct measurement of their active dynamics as free particles (cf. SI Fig 1a). The active energies, characterized from the magnitude of the free active colloid velocity following the formulation of the swim pressure described by Takatori et al. [28], are listed in SI Fig1b.

Confocal microscopy imaging of gel structure and dynamics

Gel structure and dynamics were imaged with a confocal laser-scanning microscope (Nikon A1Rsi, NA = 1.4, 100x objective). Two channels were used to image the fluorescent polystyrene (561 nm) and reflective platinum coatings (488 nm). Dynamic measurements were collected at a frame rate of 15 fps at 5 locations within the sample spaced 100 μm apart in the shape of a cross. Time series were processed using Trackpy, a Python implementation of the Crocker and Grier algorithm [29,30]. The pixel size was 83 nm for time series images and 124 nm for 3D volumes; the image size was 512 x 512 pixels and the number of slices in the 3D volumes was ~ 200. Gel structure was characterized in three dimensions using a python implementation of a watershed image analysis algorithm [31]. The uniformity of Janus colloids in the gels was confirmed by calculating the distribution of Janus particles as a function of height above the coverslip (cf. SI Figure 2). The static error in the dynamical measurements is 15 nm, as determined by the method of Savin and Doyle [32].

Rheological characterization of gels

Rheological measurements were performed with an Anton Paar MCR 702 rheometer. Passive gel rheology was characterized using a 50 mm stainless steel parallel plate with Peltier temperature controlled plate and hood. To measure active gel rheology, special care must be taken to suppress foaming of the suspension due to bubbles generated by the platinum-catalyzed decomposition of H_2O_2, SI Fig 3-5. We address this requirement by attaching polydimethylsiloxane (PDMS) films of thickness ~ 1.5 mm to the steel plates of the rheometer tooling, SI Fig 3. These PDMS films have high oxygen permeability; they

were found to prevent nucleation and growth of oxygen bubbles during active gel measurements [33], by acting as a sink for oxygen products.

PDMS films are made by mixing a 10:1 ratio of polymer to crosslinker (Dow Sylgard 182 or 184) and cured at 100°C for 4 hours in a Teflon mold [33]. The PDMS is attached with epoxy (Devcon 2 ton epoxy) to sandpaper with adhesive backing. To ensure the uniform spreading of the PDMS, a 4kg weight is placed on top during the setting period of the epoxy. The epoxy is cured for at least one hour and the PDMS-sandpaper film is attached to the steel rheometer fixtures. We compare the accuracy of the PDMS plates to traditional steel plates by measuring a frequency sweep with a solution of 4 wt. % polyethylene oxide (PEO) in water, SI Figure 6, and find no significant discrepancy between the fixtures coated with PDMS film and the standard stainless steel fixtures.

The temperature of all rheological measurements is 20°C. The strain amplitude for measurements is 0.003, confirmed to be in the linear regime (cf. Figure 2c and Figure 6) for both passive and active gels. We characterize the rheology of the passive gel with a 50 mm stainless steel fixture at a gap of 500 μm. We performed a gap study and found there are no significant gap effects above 500 μm, SI Figure 7. We chose to use a gap of 500 um to conserve sample material. A sandblasted (rough) steel fixture was used to confirm the absence of slip in the experiments of this study, SI Figure 8.

We performed oscillatory strain sweeps with PEO solutions at 1, 2, and 4 wt. % to determine the lower stress limit of the rheometer, SI Figure 11. At the strain amplitude used for all rheology measurements ($\gamma = 0.003$), the lowest resolvable modulus we can measure is G' ~ 0.01 Pa.

Microrheological characterization

The mean-squared displacement (MSD) of all particles in the gel was computed from linked trajectories determined from Trackpy. We use the generalized Stokes-Einstein equation to compute the linear viscoelastic moduli, $G'(\omega)$, $G''(\omega)$, which are extracted from a Fourier transform of the MSD at each time point following methods described in Dasgupta et al [34].

3.4 Results

The self-assembled colloidal gels are formulated with a dilute fraction of platinum coated Janus colloids dispersed uniformly in them; the Janus particles are activated by the presence of hydrogen peroxide (H_2O_2). To confirm the activity does not affect the gel structure, we image the gel structure at various levels of magnification. Figure 1 shows a 3D projection of passive and active gels imaged with a 10x, 40x, and 100x microscope objective at a t = 60 minutes after the initiation of gelation. At large magnification levels (100x), the fractal structure of the gel is present in both the passive and active gels. With progressively less magnification, the gel structure appears less fractal and instead more uniform and fluid-like, consistent with the transition from fractal to cluster structure in these gels at increasing scales [35].

In comparing the passive and active gel structures, we find the introduction of activity during gelation does not significantly affect the gel structure. Specifically, the fractal dimension of the passive gels is 1.8 ± 0.1, and their cluster size is 19 ± 5 μm. The fractal dimension of the active gels is 1.9 ± 0.1 and average cluster size is 21 ± 7 μm. The differences in d_f (p = 0.29) and R_c (p = 0.71) between active and passive gels were found to be not statistically significant.

Figure 2 shows the values of the elastic (G') and viscous (G") moduli as a function of time, frequency, and strain for a fractal cluster gel comprised of purely passive particles. Time sweeps were performed at a fixed frequency $\omega = 1$ rad/s and strain $\gamma = 0.003$. We find the gel reaches a quasi-steady state at ~ 20 minutes and G' and G" reach a plateau value of G' $= 0.15 \pm .08$ Pa and G" $= 0.13 \pm 0.06$ Pa. Colloidal gels of this kind do undergo aging; however, the time scale for our experiments (t = 15-60 min) is shorter than the timescales for aging (t $\sim$ several days) [36]. The strain sweep in Figure 2c shows the linear regime of the gel structure until $\gamma \sim 0.01$, where the gel undergoes yielding above a strain of 0.01. The addition of hydrogen peroxide to the passive gels stiffens the network by a factor of about 38%, SI Fig 10, resulting in G' $= 0.5 \pm 0.2$ and G" $= 0.3 \pm 0.2$. Such gel stiffening in the presence of H_2O_2 has been previously described [23].

Active gel rheology was characterized using the PDMS-modified rheometer fixtures. Figure 3 shows a) G' and b) G" as a function of time for H_2O_2 concentrations varying from 2.5% to 10% and for a ratio of active to passive particles at $\phi_{active} = 0.12$. We find that the introduction of activity causes a decrease in both G' and G" when compared to gels comprised of purely passive particles. The linear viscoelastic moduli furthermore decrease with increasing concentration of hydrogen peroxide. The amount of decrease is significant, with a factor of 8.5 drop in modulus relative to the passive gel observed at the highest concentration studied. These measurements in Figure 3c were acquired 30 minutes after the initiation of gelation. The modulus measured at the highest concentration of hydrogen peroxide (G' ~ 0.04 Pa) is higher than the lowest resolvable modulus determined from instrument sensitivity measurements (SI Figure 11).

To observe the effect of Janus particle fraction on the modulus change, the concentration of hydrogen peroxide is fixed at 2.5% and the active to passive particles ratio varied from 0.05 to 0.14, as reported Figure 4. Increasing the ratio of active particles also leads to a decrease in the elastic modulus of the gel network.

Because hydrogen peroxide is the fuel driving the active motion and modulus decrease, the observed effect of activity would be expected to decline as the fuel is consumed. Indeed, at extended times, the gel moduli recover and increase until they approach the values of the passive gel, which itself is undergoing aging. As reported in Figure 5, extended-time measurements of the active gels show that the active gel modulus reaches the passive gel value at about 6000 seconds. This value is consistent with expected timescales for H_2O_2 consumption, as estimated from the reaction kinetics of H_2O_2 decomposition, SI Figure 12 [6,37,38]. This correspondence corroborates the role of hydrogen peroxide, and therefore embedded activity, in the modulus change.

The following potential explanations of the measurements were evaluated and found to be incapable of explaining the observed decrease in the moduli: first, since the fractal cluster gelation process occurs with active particles present, we wondered if the activity of the Janus particles could generate different fractal cluster structures, with a weaker, lower modulus gel formed in the presence of Janus particles relative to the passive gel in which Janus particles are absent. We think this possibility is unlikely because the active and passive gel fractal cluster structures are similar, as apparent in Figure 1, and the differences in d_f and R_c for the passive and active gels are also not statistically significant.

51

A second possible explanation is syneresis accelerated by the embedded active colloids, perhaps as induced by enhanced vibrational dynamics of the active colloids. Previous work has shown that syneresis leads to the formation of a more compact gel structure with slower dynamics [36,39]. However, such behavior would lead to an increase in the modulus, which is not observed in our experiments.

Finally, an active-motion induced change in the linear region of the gels' response to small amplitude oscillatory shear could explain the measurements. All linear measurements in this study are at $\gamma = 0.003$; if active motion reduced the linear region below this value, a lower apparent modulus might be found for the active gels. Figure 6 shows there is at most a very modest shift in the onset of non-linearity for an active gel (5% H2O2) when compared to the passive gel ($\gamma_{passive} = 0.07$ vs. $\gamma_{active} = 0.03$); however the strain used for our measurements ($\gamma = 0.003$) remains well within the linear elastic region of the active gel.

To generalize our results to any active particle system – and not specifically to one in which the activity is generated by platinum-catalyzed decomposition of hydrogen peroxide – we plot the modulus as a function of the energy of the active colloids, E_A. The energy of an active colloid is given by: $E_A = \xi Vl$, where ξ is the hydrodynamic drag, V is its velocity, and l is the run length of an active particle, given by $l = \tau_R V$. The active particle run length is a function of V and the Brownian reorientation time, $\tau_R = \frac{8\pi\eta a^3}{k_B T}$, where η is the viscosity of the solvent and a is the particle radius [23,28]. Over the range of H_2O_2 concentrations used in this study, we find that each active particle engages in dynamics equivalent to an energy that is $3 - 9$ times greater than the system's thermal

energy (cf. SI Figure 1b). This approach has been previously applied to characterize the microdynamics of active gel networks [23].

To account for the joint effects of the ratio of active colloids and the H_2O_2 concentration, we plot G' and G" as a function of $N_A E_A / N_P E_P$ where N_A / N_P is the ratio of active to passive colloids and E_A / E_P is the additional energy of the active colloids.

$$\frac{N_A E_A}{N_P E_P} = \frac{\xi V^2 \tau_R}{k_B T} \tag{2}$$

Figure 7 shows G' and G" as a function of the inputted active energy, $N_A E_A / N_P E_P$. The contributions from both the ratio of active to passive particles and the energy of the active particle collapse on to a single curve, and the modulus of the gel network decreases with increasing energy provided by the active colloids.

To probe whether the decrease in the gel modulus is correlated to a change in microscopic dynamics of the gel network, we use microrheology to compute the frequency-dependent modulus at various times after initiation of gelation. We compute the ensemble averaged mean squared displacement (MSD) of the gel network, $< x^2(\tau) >$, at 0, 15, 30, and 60 minutes after addition of salt to induce particle gelation, shown in Figure 8. The MSD of the gel network increases with an increase in the H_2O_2 concentration, consistent with previous reports [23]. The increase in the MSD with increasing active energy correlates with a decrease in the values of the frequency dependent elastic modulus determined from microrheology, Figure 8.

We compare the values of G'(ω) and G"(ω) obtained from microrheology and macroscopic rheological measurements at 15 minutes after the addition of salt. This time point was chosen to allow sufficient time for gelation while also ensuring that the H_2O_2 driving the active motion had not been significantly consumed. The frequency sweeps

performed with mechanical rheology, shown in Figure 9, were measured by allowing the gel to equilibrate quiescently on the rheometer for 15 minutes, followed by execution of a frequency sweep. Frequency sweeps as characterized through mechanical rheology showed the decrease in the viscoelastic moduli due to activity holds over a wide frequency range.

Comparison of the frequency-dependent moduli reveals a discrepancy in the micro and macro rheology; specifically, figure 10 shows that the moduli obtained from microrheology are higher than the mechanical rheology values for both a) passive and b) active gels with 5% H_2O_2 (E_a/E_p = 3.8). The differences between microrheology and mechanical rheology of the passive gels is greatest at high frequencies. The low frequency (in the range 0.5-1 s^{-1}) averages 20%; the discrepancy at high frequencies (in the range 2-10 s^{-1}) averages 42%. Overall the average discrepancy between the microrheological prediction and the mechanical rheology is 34%.

The discrepancy for the passive fractal gels can be attributed to the following possibilities: (i) failure of the generalized Stokes-Einstein equation to quantitatively describe the rheological response of the gel; (ii) variation of the gel structure itself during the ~ 4 min measurement period. With respect to the second explanation, we do find some hysteresis in the mechanical rheology when the measurements are performed in the order of increasing vs decreasing frequency (c.f SI Figure 13). Moreover, for passive gels formed 60 minutes after addition of salt (when the gel structure has reached quasi steady-state) we find that the modulus obtained from microrheology matches the values measured on the rheometer to a much higher degree. In SI Fig 14, the average discrepancy for the data over the full frequency range is 9%.

Figure 10c shows the ratio of the moduli determined from micro and macro rheology, over the full frequency range. As discussed in the previous paragraph, for passive gels, the amount of overprediction of microrheology is as large as a factor of 2.0 for G' and 3.0 for G"; however, at low frequencies there is a smaller discrepancy between microrheology and mechanical rheology. The discrepancy between the viscoelastic moduli determined from the two methods is much larger for the active gels. The amount of overprediction by microrheology is larger for active gels, up to a factor of 5.0 for G' and G".

To proceed with further analysis, we note that the passive gel microrheology and mechanical rheology agree relatively well at low frequencies (discrepancy less than 20% for all frequencies less than 1 s^{-1}). The low-frequency condition is broken out therefore for further analysis of the effect of H_2O_2 conditions on the degree of modulus change. To that end, figure 11a shows G' and G" as a function of H_2O_2 concentration at a fixed frequency (0.5 s^{-1}), obtained from micro and macro rheology. The mechanical rheology measurements show a greater decrease in the modulus with increasing H_2O_2 concentrations, and the microrheology overestimates the modulus obtained from mechanical rheology at all H_2O_2 concentrations. Figure 11b shows a ratio of the modulus obtained from micro and mechanical rheology ($\omega = 0.5$ s^{-1}) as a function of $\%H_2O_2$. At low H_2O_2 concentrations, the ratio is consistent with the additional energy of the active colloids; however with increasing active energy, the ratio is less than the amount of active energy input into the system by the Janus particles.

3.5 Discussion

Embedded active colloids decrease the linear viscoelastic moduli of a fractal cluster colloidal gel. The amount of decrease is a function of the total active energy input, which is itself dependent on the ratio of active to passive colloids and the energy of the active Janus particles. The active energy of the Janus particles is set by the concentration of H_2O_2. At long times, after the Janus particles have consumed the H_2O_2 and their activity is no longer significant, the linear viscoelastic moduli of the gel network assumes levels observed for passive gels. These experimental measurements and estimates of reaction kinetics for H_2O_2 decomposition indicate that H_2O_2 is present until at least t ~ 10^3 sec. The magnitude of the moduli decrease due to the embedded active colloids is significant: At an active particle concentration of only ~ 10%, the moduli decrease by a factor of 8.5.

We furthermore compare the frequency-dependent moduli of the gels, as measured by microrheology and mechanical rheometry. The purpose of this comparison is to assess the validity of the fluctuation-dissipation theorem in the present case, which connects microscopic fluctuations to macroscopic properties for systems in equilibrium. This theorem is the basis for microrheology through its role in the generalized Stokes-Einstein equation. The two methods agree well for passive gels at low frequencies, consistent with the generalized Stokes-Einstein equation.

Both methods – microrheology and mechanical rheometry – show a decrease in the modulus with increasing activity across a wide range of frequencies. However, the microrheology measurements – the theory of which assumes validity of the fluctuation dissipation theorem – overestimates the mechanically measured moduli of the active gels over all H_2O_2 concentrations studied. The energy scale in the generalized Stokes-Einstein

equation is the thermal energy of Brownian motion, k_BT; however, an active particle's energy is enhanced by a factor of $3 - 9$ times k_BT across the range of H_2O_2 concentrations studied. If the dilute concentration of active colloids is factored in, the overall energetic increase of the gel due to activity is a factor of 1.2. (This factor is: $1 + \frac{N_A E_A}{(N_A + N_B)k_B T}$). Substituting E_a in place of k_BT in the generalized Stokes-Einstein equation yields an even larger discrepancy between microrheology and mechanical rheology measurements, SI Figure 15.

This discrepancy between microrheology and mechanical rheometry is confirmation of the hypothesis that the fluctuation – dissipation theorem is not applicable to these active gels. This conclusion is not surprising because the active system is out of equilibrium. The opportunity that the present measurements offer is to explore the exact nature of the failure: because of the availability of both microscopic and macroscopic rheological characterization, this work places bounds on the out-of-equilibrium relationship that connects the microscopic fluctuations in the active gel system to the measured rheology.

In previous work, active actin gels were shown to violate the fluctuation dissipation theorem due to contractile forces the myosin motors apply to the actin network [11]. In these gels, myosin motors act as active crosslinks making the gels more rigid [11,12]. Studies of active gels concluded that the activity of the myosin motors leads to contraction and stiffening of the active actin gels – equivalent to a modulus enhancement. In this study, we find that fractal cluster gels with embedded active particles display opposite behavior. That is, the active particles embedded within colloidal gels lead to a softening of the gel network. The opposite trend in the two systems (modulus decrease vs

increase) is likely due to the differences between their sources of the activity and how they interact with the passive network structure in which they have been incorporated. Myosin motors are able translate along the actin filaments and alter the structure of the actin gels; whereas, in our active gels, the active particle is bound to the gel network through attractive forces that are stronger than the active energy.

We explore several potential mechanisms that describe the origin of the decrease in the moduli with activity in the fractal cluster gels. We conceptualize possible effects of active motion into two primary categories: one in which the active motion changes the gel network itself and the other in which active motion acts to change dynamical features of the gel network. As discussed in the results, changes in the structure of the gel network, including variations in the fractal structure and accelerated syneresis, were not observed in our experiments. We do observe an (at most) modest shift in the onset of non-linearity for active gels. However, all measurements were performed at low enough strain amplitudes ($\gamma = 0.003$) to afford high confidence of their linearity.

The embedded active colloids could also change the modulus of the gel by acting to change the dynamics of the gel network. Potential mechanisms include the actin gel scenario, where the active motion induces a tension on the network. The tension induced on actin gel networks results in stiffening – an increase in the viscoelastic moduli, which is not observed in our gels.

The change in the modulus could also arise from a combination of active motion effects on microdynamics with the breakdown of the fluctuation dissipation theorem. Specifically, in prior work the enhanced microdynamics of the fractal cluster gels with embedded active particles was modeled as the sum of the three contributions. The first is

the contribution due to passive motion; the second is a direct contribution to the overall mean squared dynamics from the active motion of the embedded particles; the third is an indirect contribution, in which the active dynamics of the embedded Janus particles increase the dynamics of neighboring passive particles, because of their coupling to the fractal cluster structure. If this effect is coupled with the hypothesis that the enhanced microdynamics yield a modulus decrease through an as yet unknown modification of the fluctuation dissipation theorem, the modulus decrease would be explained.

Additional mechanisms that could explain the change in the modulus include the effects of enhanced osmotic pressure or changes in the effective spring constant between colloidal bonds. We here explore each idea in turn.

First, previous theories of active particles presented by Takatori et. al. describe the swim pressure of active colloids, which leads to swelling [40]. The active colloids embedded within the gel network could increase the effective osmotic pressure in the system, which could have implications on the modulus.

Second, the active motion could also cause a reduction in the effective spring constant between colloidal bonds. In this potential mechanism, the increased vibrations of particles within the gel due to active motion leads to an increase in the average separation distance between a pair of colloidal particles. As a result, the bonds are longer where the pair potential has a weaker attraction causing a reduction in the spring constant. The weakening of the attraction and reduction of the spring constant could increase the active gel microdynamics, and induce a decrease in the modulus of the gel network [41].

Here we focused on macroscopic measurements of the elastic and viscous modulus of active colloidal gels as a function of time and frequency at a fixed strain

amplitude. Having found that there is a significant decrease in the modulus of the gel, future work might address how activity affects other rheological properties, such as yielding or the steady shear behavior. Future work could also address the extension of the generalized Stokes-Einstein relation to active colloidal suspensions.
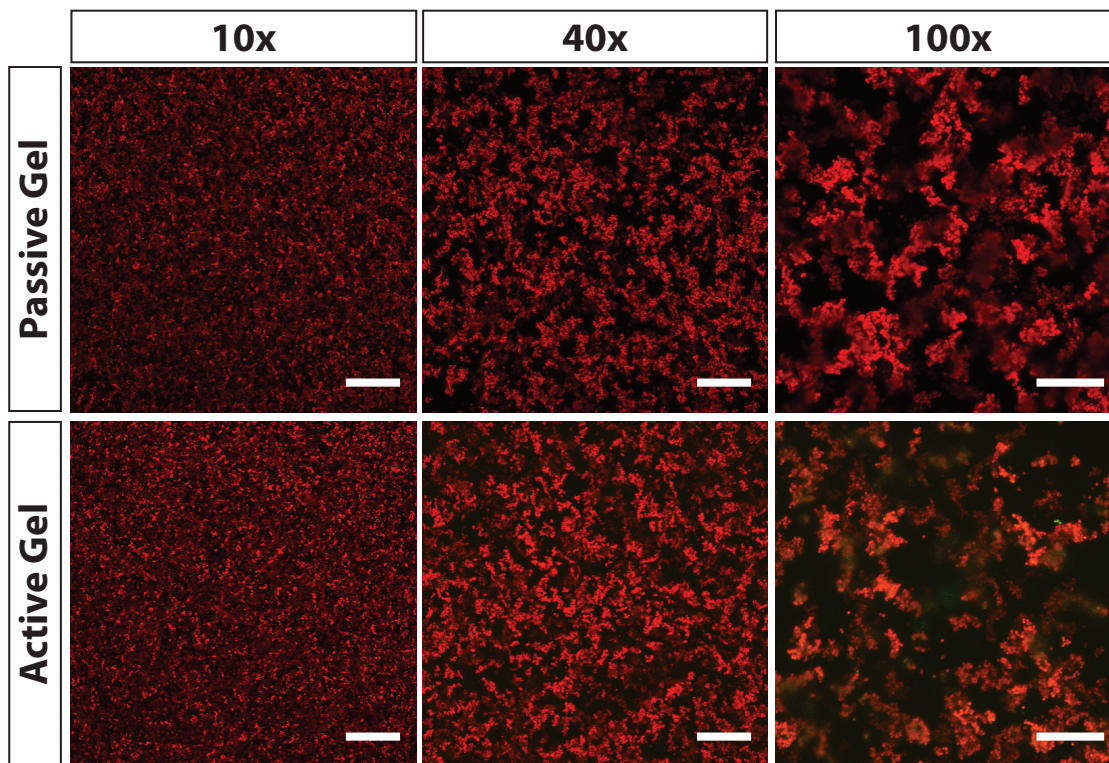
3.6 Acknowledgements

Figure 3-1. Passive and active gel structure across multiple length scales 60 minutes after initiation of gelation. Scale bar for 10x objective is 200 μm, 40x objective is 50 μm, and 100x objective is 25 μm.
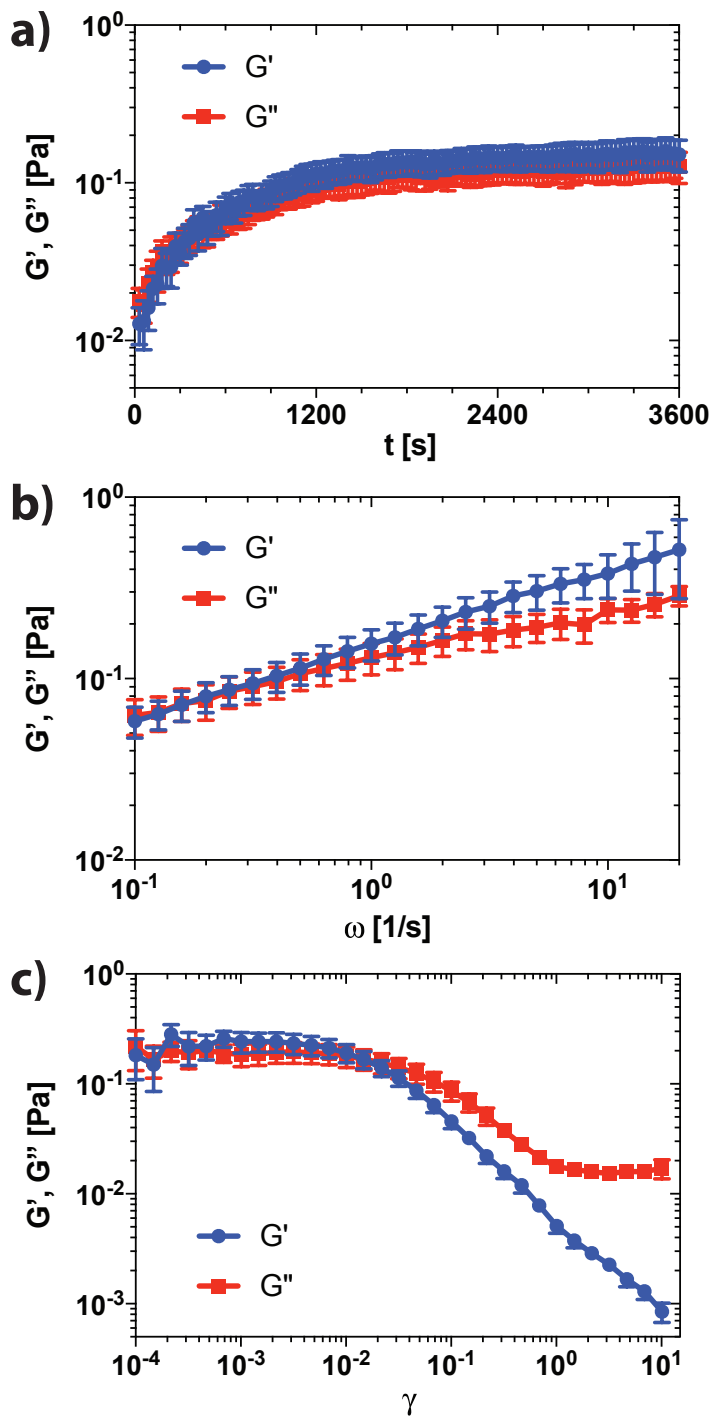
Figure 3-2. Passive gel rheology as a function of a) time, $\gamma = 0.003$ and $\omega = 1$ s^{-1}, b) frequency, $\gamma = 0.003$, and c) strain, $\omega = 1$ s^{-1}.
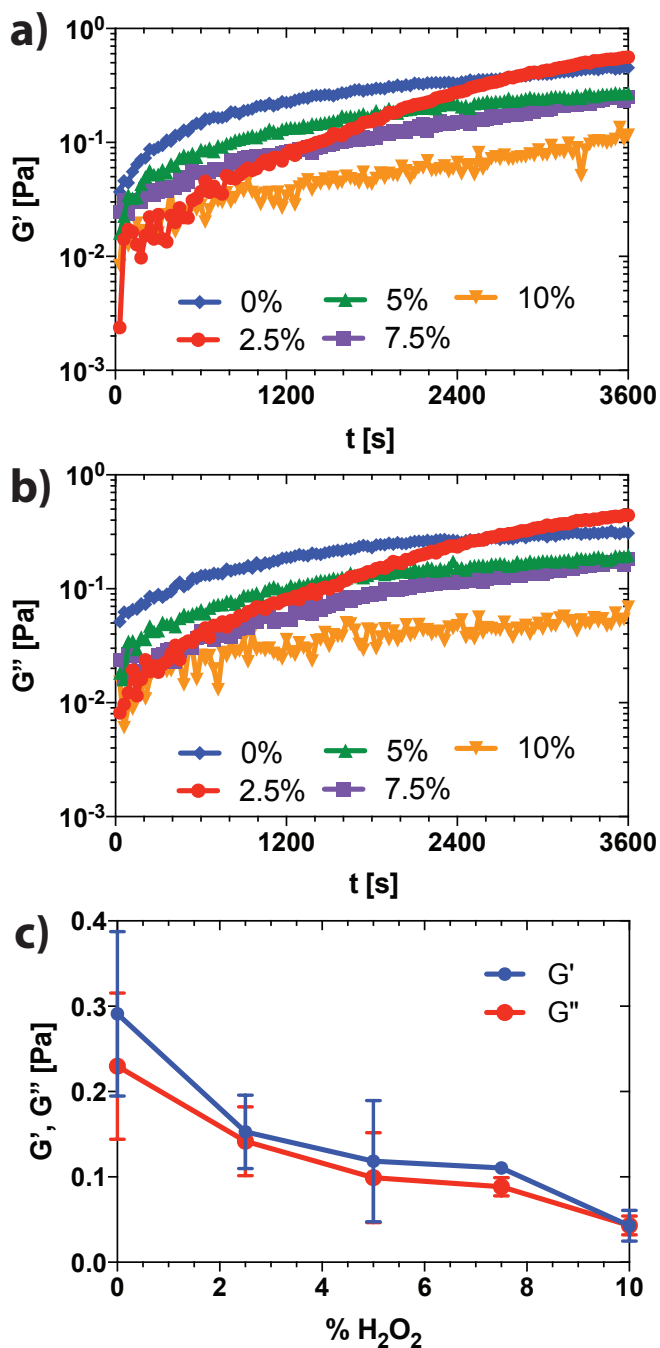
Figure 3-3. Active gel rheology at a fixed ratio of active to passive particles (ϕ_{Active} = .12) varying the concentration of hydrogen peroxide. a) Elastic and b) viscous moduli as a function of time at each H_2O_2 concentration. c) G', G" as a function of the H_2O_2 concentration at a fixed time t = 1800 s. Measurements were performed at a fixed strain (γ= 0.003) and frequency (ω = 1 s^{-1}).
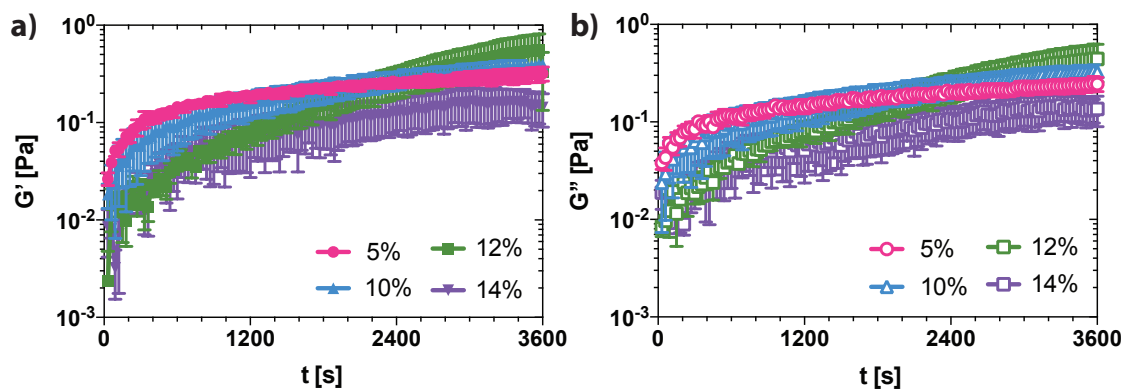
Figure 3-4. Active gel time sweep at fixed concentration of hydrogen peroxide (2.5%) varying the ratio of active to passive particles. a) Elastic and b) viscous moduli as a function of time at a fixed strain (γ= 0.003) and frequency (ω = 1 s^{-1}).
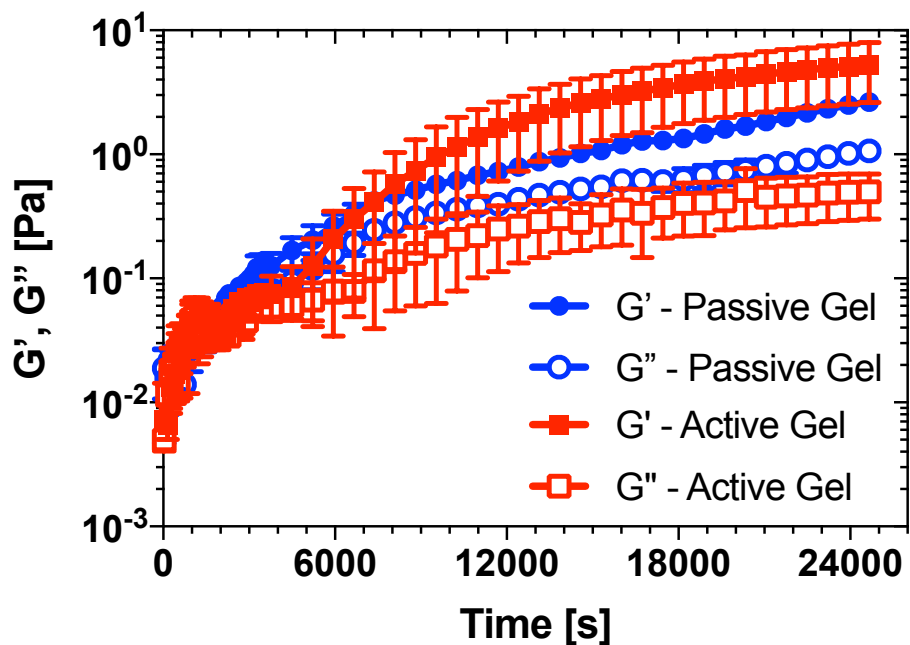
Figure 3-5. Long time study of active gels. Time sweep of passive gels and active gel (5% H2O2 added) for 7 hours at a fixed strain (γ = 0.003) and frequency (ω = 1 s^{-1}). Active gel reaches modulus of passive gel around t = 6000 s after H_2O_2 is depleted.
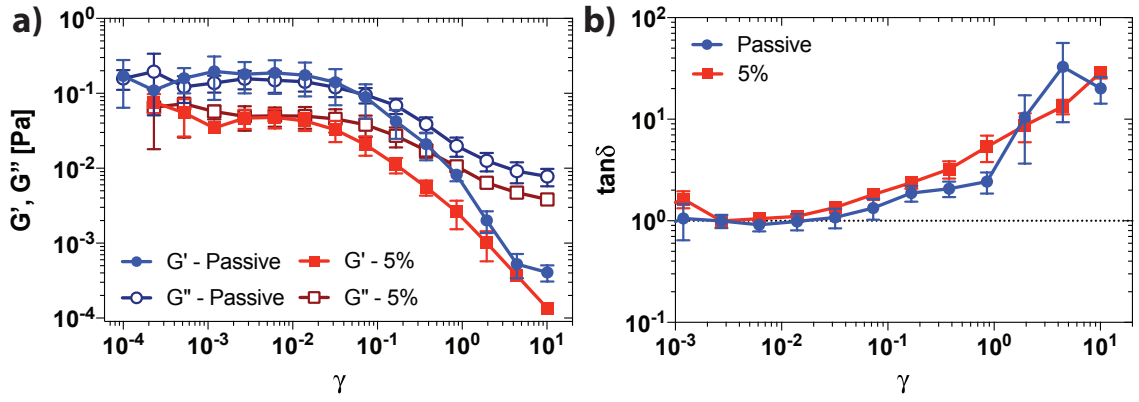
Figure 3-6. Strain sweep of passive and active gel, with 5% H_2O_2. a) G' and G" and b) tan δ as a function of strain at a fixed frequency, ω = 1 s^{-1}. Strain sweep shows a small shift in the onset of non-linearity for active gels.
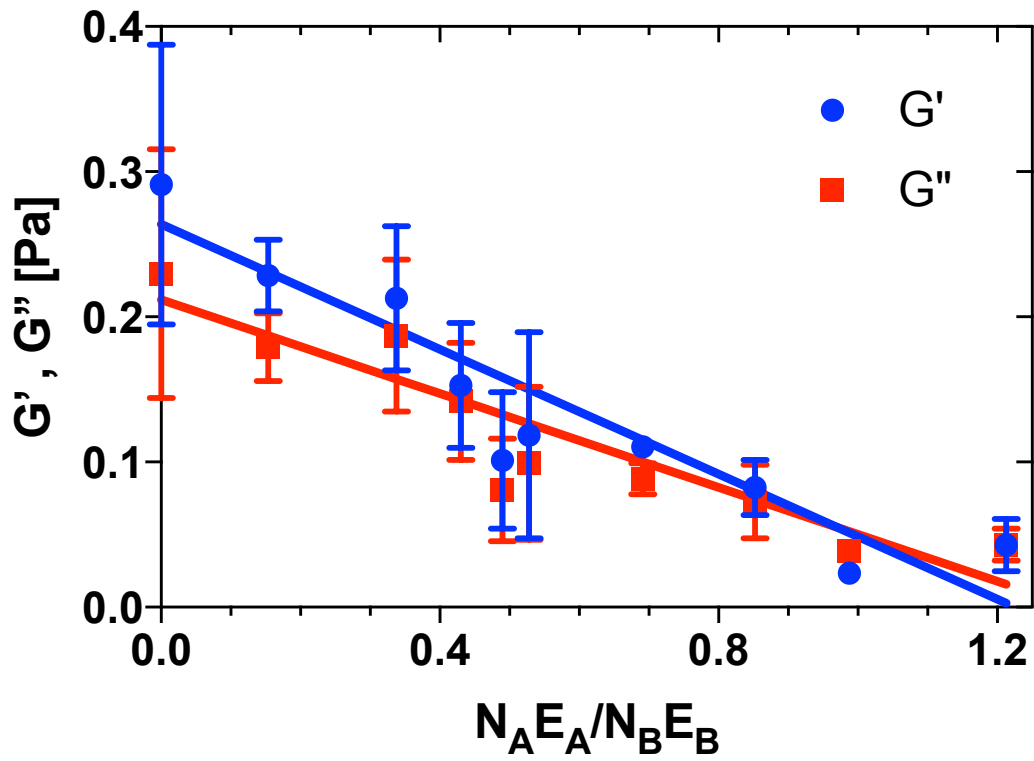
Figure 3-7. Viscoelastic moduli as a function of the total inputted active energy (γ = 0.003, ω = 1 s^{-1}, t = 1800 s).
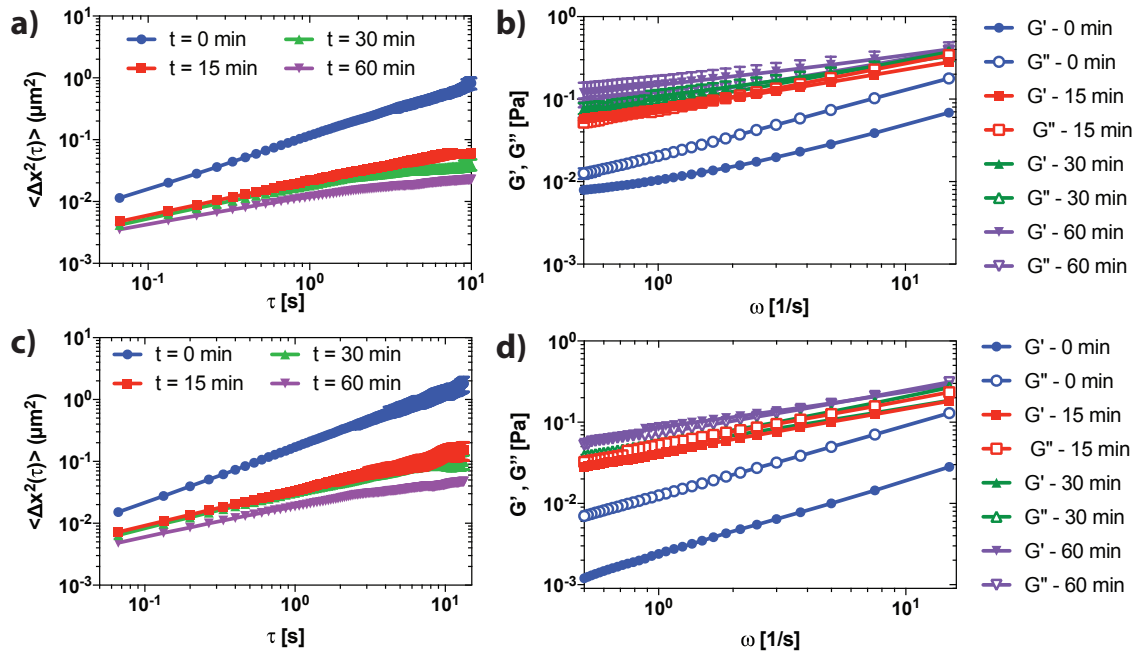
Figure 3-8. Microdynamics and microrheology of passive and active gels. Mean squared displacement of a) passive and c) active gels at t = 0, 15, 30, and 60 minutes after addition of salt to induce gelation. Microdynamic measurements are converted to frequency dependent viscoelastic moduli for b) passive and d) active gels using a generalized Stokes-Einstein equation.
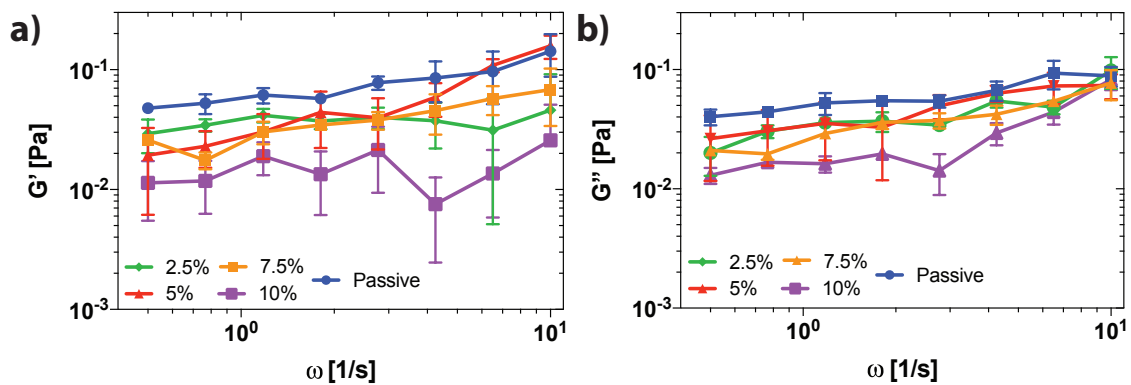
Figure 3-9. Frequency sweeps of passive and active gels. Active gels have a fixed ratio of active to passive colloids and 2.5%, 5.0%, 7.5% or 10% H_2O_2 ($\gamma = 0.003$, t = 900 s).
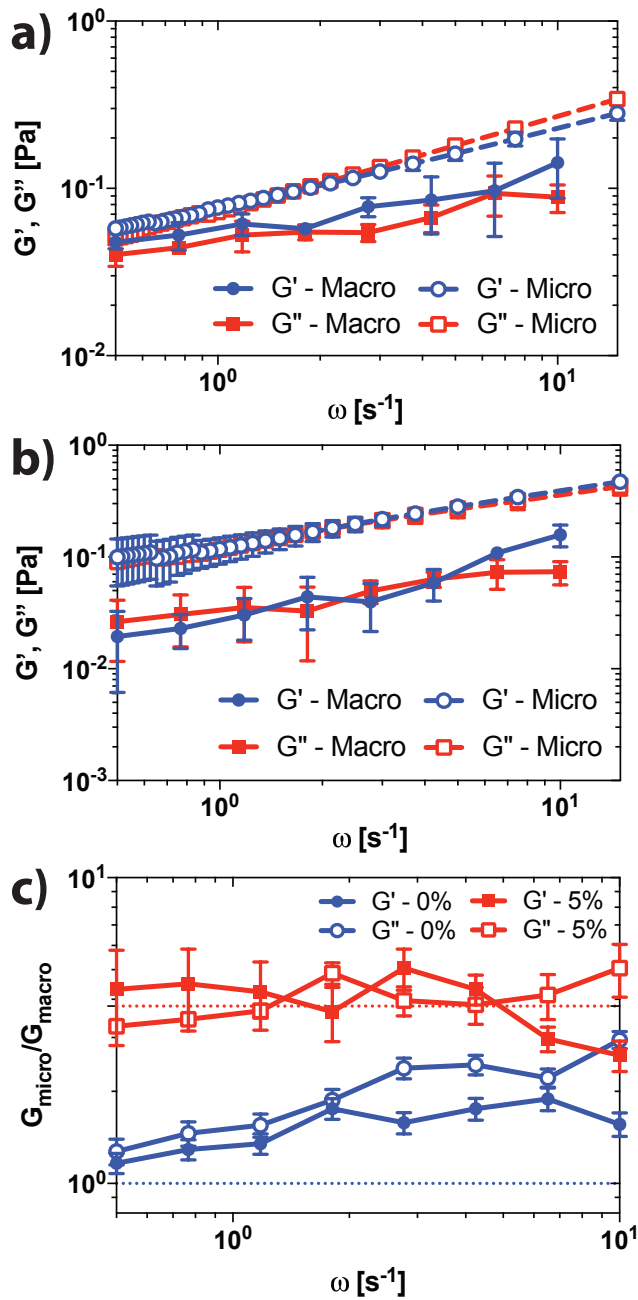
Figure 3-10. Comparing frequency dependent G' and G" obtained from micro and macro rheology for a) passive and b) active gel with 5% H_2O_2. Micro and macro rheology frequency sweeps were collected 15 minutes after addition of salt to allow sufficient time for particle gelation. c) Ratio of G' and G" obtained from microrheology and mechanical rheology as a function of frequency.
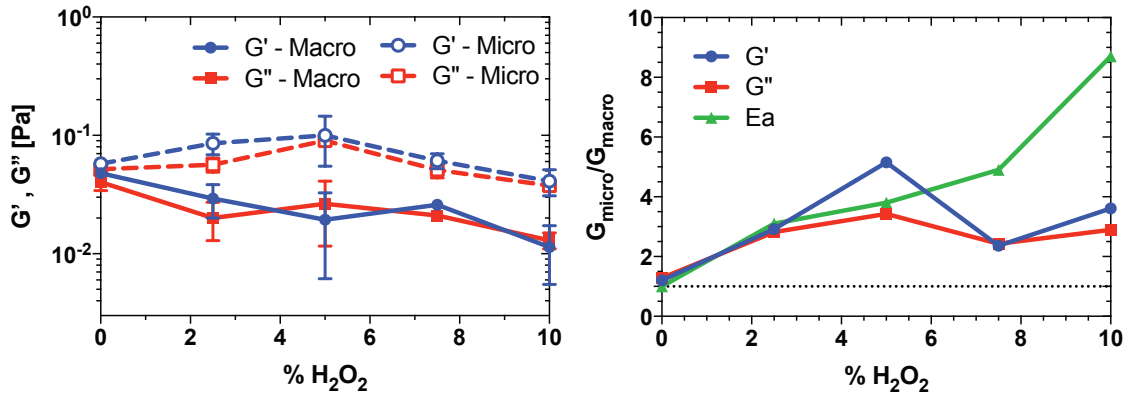
Figure 3-11. Comparison of viscoelastic moduli obtained from microrheology and mechanical rheology at a fixed frequency ($\omega = 0.5$ s^{-1}) as a function of the hydrogen peroxide concentration. a) Viscoelastic moduli and b) ratio of moduli obtained from microrheology and mechanical rheology with active energy as a function of hydrogen peroxide concentration.
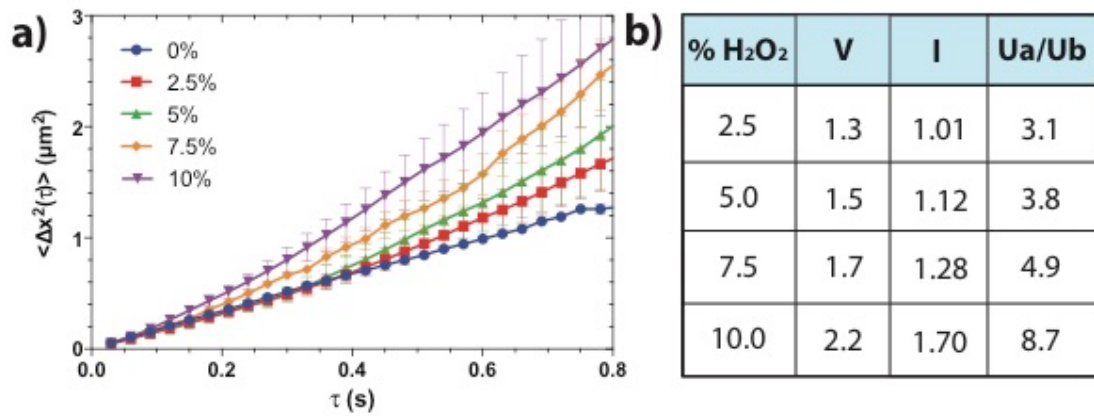
3.7 Supplemental Information

Figure 3S-1. Microdynamics and energy of free active colloids. a) Mean squared displacement of free active colloids at each hydrogen peroxide concentration. b) Velocity (V), run length (l), and active energy (Ua/Ub) at each hydrogen peroxide concentration. Velocity is shown in units $\mu m/s$ and run length is shown in μm.
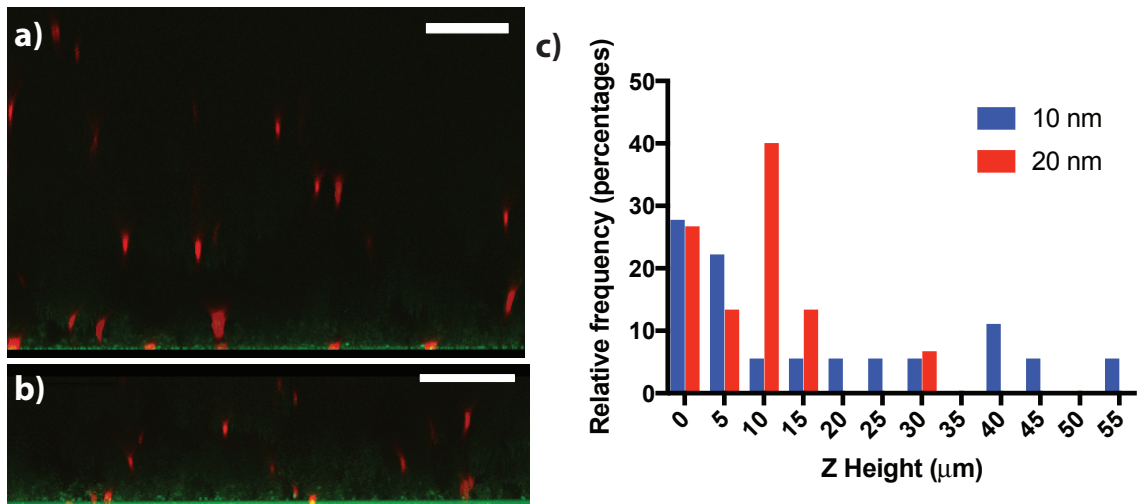
Figure 3S-2. Distribution of Janus particles in gel samples. XZ image of Janus particles in gel samples with a) 10 nm and b) 20 nm of Platinum coated on Janus particle. c) Relative frequency of Janus particles as a function of z height with 10 and 20 nm of Platinum. Janus particles with 10 nm Platinum coated are more evenly distributed throughout the gel network than thicker Platinum coating.
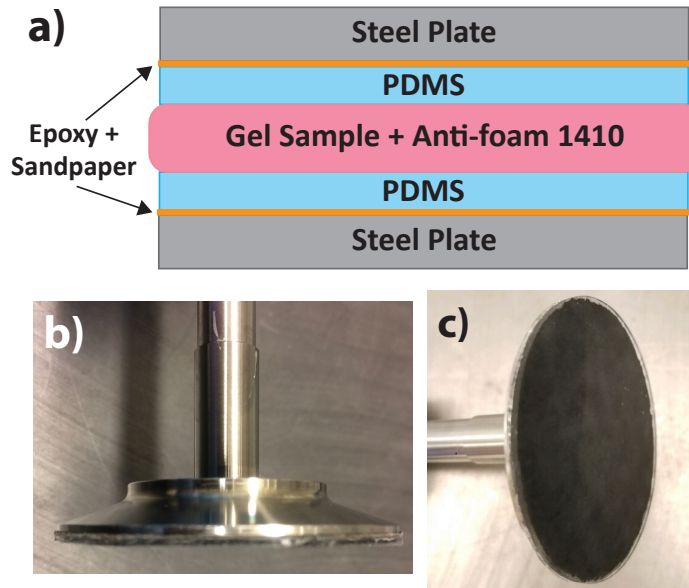
Figure 3S-3. Design of PDMS plates for active gel rheology experiments. a) Schematic of PDMS plate attached to steel fixture using epoxy and sandpaper with adhesive back. PDMS is attached to sandpaper with adhesive back using Devcon 5 minute epoxy. Photographs of PDMS attached to 50 mm stainless steel fixture shown in b) and c).